

Electronic Supplementary Information

Direct Observation of Cu^I/Cu^{III} Redox Steps Relevant to Ullmann-Type Coupling Reactions

Alicia Casitas, Amanda E. King, Teodor Parella, Miquel Costas, Shannon S. Stahl,*
Xavi Ribas*

CONTENTS

1. Supplementary methods	S2
1.1. Materials and methods.....	S2
1.2. Instrumentation.....	S2
1.3. Synthesis and characterization of aryl-Cu ^{III} -halide complexes.....	S2
1.4. Synthesis and characterization of C-X coupling products.....	S4
1.5. Crystallographic characterization of aryl-Cu ^{III} -halide complexes.....	S6
1.6. General Procedure for Monitoring Catalytic Coupling of L₁-Br with Pyridone by NMR Spectroscopy	S7
2. Supplementary Figures	S8
3. Supplementary Tables.....	S35
4. Supplementary Notes	S38

1. Supplementary Methods

1.1. Materials and methods

Reagents and solvents used were commercially available reagent quality unless indicated otherwise. Solvents were purchased from SDS and were purified and dried by passing through an activated alumina purification system (MBraun SPS-800). Preparation and handling of air-sensitive materials were carried out in a N₂ drybox (MBraun-Unilab) with O₂ and H₂O concentrations < 1 ppm. Ligands L₁ and L₂ were synthesized following published procedures.^{1,2}

1.2. Instrumentation

UV-vis spectroscopy was performed on a Cary-50 (Varian) UV-vis spectrophotometer. Low temperature control was maintained with a cryostat from Unisoku Scientific Instruments, Japan. NMR data concerning product identity were collected on Bruker 600 MHz, Bruker 500 MHz or Bruker 400 MHz AVANCE spectrometers in DMSO, CDCl₃ or CD₃CN and calibrated relative to an internal reference, either the residual protons of the solvent or added tetramethylsilane. NMR data concerning the catalytic coupling of L₁-Br with pyridone were collected on a Bruker AC 300 MHz spectrometer. C, H, N elemental analyses were performed on a ThermoFinnigan Flash-EA1112 analyzer. ESI-MS experiments were collected and analyzed on a Bruker Daltonics Esquire 6000 spectrometer with acetonitrile or acetonitrile/water (80:20) as the mobile phase. Cyclic voltammetry (CV) experiments were performed in an IJ-Cambria HI-660 potentiostat using a three electrode cell. Glassy carbon disk electrodes (3mm diameter) from BAS were used as working electrode, platinum wire was used as auxiliary and SSCE electrode as the reference.

1.3. Synthesis and characterization of aryl-Cu^{III}-halide complexes

Complexes **1_{Cl}**, **1_{Br}**, **2_{Cl}** and **2_{Br}** were prepared by following a procedure analogous to that described previously for the preparation of the [aryl-Cu^{III}](ClO₄)₂ complex,¹ using ligand L₁ (for **1_{Cl}**, **1_{Br}**) or L₂ (for **2_{Cl}**, **2_{Br}**) (1.1 equiv) and CuX₂ (X=Cl, Br). The solid was recrystallized in CH₃CN (**1_{Cl}**) or DMF (**1_{Br}**, **2_{Br}**, **2_{Cl}**) by slow diethyl ether diffusion over the resultant solution, affording crystals of the desired complexes.

Complexes **1_I** and **2_I** were prepared by dropwise addition of a solution of AgClO₄ (2 equiv) in CH₃CN to a vigorously stirred solution of [L₁C-CuCl]Cl (**1_{Cl}**) or [L₂C-CuCl]Cl (**2_{Cl}**) in CH₃CN respectively. After a few seconds the solution became cloudy

and a precipitate appeared. The solution is filtered through Celite and then through an Acrodisc® filter. The resultant solution is added dropwise to a stirred solution of KI (2 equiv) in CH₃CN (1 mL). After 10 minutes stirring, slow diethyl ether diffusion over the final solution dark green crystals corresponding to complexes **1_I** and **2_I** respectively.

1_{Cl}. Anal. Calcd for [L₁C-Cu^{III}Cl]Cl (%) 47.31 C, 11.03 N, 6.35 H; found: 47.01 C, 11.02 N, 6.14 H. ¹H-NMR (DMSO-D₆, 500MHz) δ, ppm: 8.16 (s, 2H), 7.14 (t, J=7.4Hz, 1H), 6.89 (d, J=7.4Hz, 2H), 4.37(dd, J=15.3Hz, J=5.6Hz, 2H), 4.16 (dd, J=8.5Hz, J=15.3Hz, 2H), 3.21 (t, J=13Hz, 2H), 3.11 (t, J=12.7Hz, 2H), 2.80 (s, 3H), 2.72 (d, J=11Hz, 2H), 2.30 (d, J=12.7Hz, 2H), 2.03 (q, J=13Hz, 2H), 1.80 (d, J=16Hz, 2H). ¹³C-NMR (DMSO-D₆, 500MHz), δ, ppm: 179.7 (C1), 146.1 (C2), 128.3 (C4), 121.8 (C3), 61.7 (C5), 57.8 (C6), 51.2 (C8), 40.7(C9), 23.1 (C7). ESI-MS (CH₃CN, m/z): 345(100) [C₁₅H₂₄CuClN₃]⁺.

1_{Br}. Anal. Calcd for [L₁C-Cu^{III}Br]Br (%) 38.35 C, 8.94 N, 5.14 H, found: 38.05 C, 8.65 N, 4.84 H. ¹H-NMR (CH₃CN, 400MHz) δ, ppm: 7.98 (s, 2H), 7.13 (t, J=7.4Hz, 1H), 6.92 (d, J=7.4Hz, 2H), 4.35 (dd, J=19.6Hz, J=5.6Hz, 2H), 4.15 (dd, J=15.6Hz, J=8.8Hz, 2H), 3.35 (m, 2H), 3.17 (t, J=12.4Hz, 2H), 2.79 (s, 3H), 2.66 (d, J=10.4Hz, 2H), 2.38 (d, J=12.8Hz, 2H), 2.02 (q, J=8.4Hz, 2H), 1.83(d, J=Hz, 2H). ¹³C-NMR (DMSO-D₆, 400MHz) δ, ppm: 181.31 (C1), 146.29 (C2), 128.81 (C4), 122.44 (C3), 62.21 (C5), 58.38 (C6), 51.57 (C8), 41.19 (C9), 23.58 (C7). ESI-MS (CH₃CN, m/z): 390.0(100) [C₁₅H₂₄CuBrN₃]⁺.

1_I. (yield: 84%) Anal. Calcd for [L₁C-Cu^{III}I]I (%) 31.96 C, 7.45 N, 4.29 H, found: 31.65 C, 7.38 N, 4.36 H. ¹H-NMR (CD₃CN, 300MHz) δ, ppm: 7.11 (t, J=7.5Hz, 1H), 6.86 (d, J=7.5Hz, 2H), 6.58 (s, br, 2H), 4.28 (dd, J=15Hz, J=5.1Hz, 2H), 4.17 (dd, J=15Hz, J=8.1Hz, 2H), 3.50 (q, J=12.8Hz, 4H), 2.85 (s, 3H), 2.52 (tt, J=12.9Hz, J=3.3Hz, 4H), 2.27(m, 2H), 1.89(m, 2H). ¹³C-NMR (CD₃CN, 300MHz) δ, ppm: 182.47 (C1), 145.14 (C2), 128.50 (C4), 122.19 (C3), 61.68 (C5), 59.04 (C6), 50.99 (C8), 42.16 (C9), 23.41 (C7). ESI-MS (CH₃CN, m/z): 436.0(100) [C₁₅H₂₄CuIN₃]⁺.

2_{Cl}. Anal. Calcd for [L₂C-Cu^{III}Cl]Cl·H₂O (%) 43.69 C, 10.92 N, 6.29 H, found: 43.76 C, 10.93 N, 6.32 H. ¹H-NMR (DMSO-D₆, 500MHz) δ, ppm: 7.42 (s, 2H), 7.11 (t, J=7Hz, 1H), 6.88 (d, J=7Hz, 2H), 4.36 (dd, J=15Hz, J=5Hz, 2H), 4.17 (dd, J=14Hz, J=9Hz,

2H), 4.17 (s, 1H), 3.04 (q, $J=12\text{Hz}$, 2H), 2.75 (m, 6H), 1.85 (d, $J=15\text{Hz}$, 2H), 1.72 (q, $J=13\text{Hz}$, 2H). $^{13}\text{C-NMR}$ (DMSO-D₆, 500MHz) δ , ppm: 179.66 (C1), 145.53 (C2), 127.97 (C4), 121.59 (C3), 61.91 (C5), 51.27 (C6), 48.14 (C8), 26.21 (C7). ESI-MS (DMSO:CH₃CN, m/z): 330.1(100) [C₁₄H₂₂CuClN₃]⁺.

2_{Br}. Anal. Calcd for [L₂C-Cu^{III}Br]Br·1.5DMF (%) 29.74 C, 7.43 N, 3.92 H, found: 29.39 C, 7.37 N, 3.80 H. $^1\text{H-NMR}$ (CH₃CN, 400MHz) δ , ppm: 7.23 (s, 2H), 7.10 (t, $J=7.2\text{Hz}$, 1H), 6.89 (d, $J=7.2\text{Hz}$, 2H), 4.32 (dd, $J=15.2\text{Hz}$, $J=5.6\text{Hz}$, 2H), 4.14 (dd, $J=15.2\text{Hz}$, $J=9.2\text{Hz}$, 2H), 4.10 (s, 1H), 3.05 (q, $J=11.2\text{Hz}$, 2H), 2.74 (m, 6H), 1.86 (d, 15.6Hz, 2H), 1.69 (m, 2H). $^{13}\text{C-NMR}$ (DMSO-D₆, 400MHz) δ , ppm: 180.00 (C1), 145.74 (C2), 128.46 (C4), 122.19 (C3), 62.41 (C5), 51.60 (C6), 48.84 (C8), 26.71 (C7). ESI-MS (DMSO:CH₃CN, m/z): 376.0(100) [C₁₄H₂₂CuBrN₃]⁺.

2_I. (yield: 98%) Anal. Calcd for [L₂C-Cu^{III}I]I (%) 30.59 C, 7.64 N, 4.03 H, found: 30.33 C, 7.31 N, 3.82 H. $^1\text{H-NMR}$ (CD₃CN, 400MHz) δ , ppm: 7.08 (t, $J=7.4\text{Hz}$, 1H), 6.83 (d, $J=7.4\text{Hz}$, 2H), 6.16 (s, 2H), 4.18 (m, 4H), 3.76 (s, 1H), 3.12 (m, 4H), 2.93 (d, $J=11.6\text{Hz}$, 2H), 2.54 (d, $J=12\text{Hz}$, 2H), 1.99 (m, 4H). $^{13}\text{C-NMR}$ (CD₃CN, 400MHz) δ , ppm: 179.17 (C1), 144.36 (C2), 128.14 (C4), 122.12 (C3), 61.80 (C5), 51.02 (C6), 49.51 (C8), 26.13 (C7). ESI-MS (CH₃CN, m/z): 421.8(100) [C₁₄H₂₂CuIN₃]⁺.

1.4. Synthesis and characterization of C-X coupling products

L₁-Cl. Under N₂ atmosphere, 2 equivalents of acid (CF₃SO₃H, 0.023 M, 1.4 mL, 0.032 mmols) are added dropwise to a stirred solution of complex **1_{Cl}** (6.1 mg, 0.016 mmols) in previously deoxygenated CH₃CN (3 mL), causing a color change from red to colorless in seconds (100% NMR yield). NH₄OH (1 mL, 28% in water) is added to the solution and the organic product is extracted with CH₂Cl₂. The organic phase is dried with MgSO₄ and then dried under vacuum overnight to obtain a yellow oil. $^1\text{H-NMR}$ (CDCl₃, 400MHz) δ , ppm: 7.14 (m, 3H, H^a, H^b), 4.40 (d, $J=14\text{Hz}$, 2H, H^c or H^d), 3.53 (d, $J=14.4\text{Hz}$, 2H, H^c or H^d), 2.39 (m, 4H, H^e or H^f, Hⁱ or H^j), 2.31 (m, 2H, H^e or H^f), 2.01 (m, 2H, Hⁱ or H^j), 1.86 (s, 3H, CH₃), 1.46 (m, 4H, H^g, H^h). $^{13}\text{C-NMR}$ (CDCl₃, 400 MHz) δ , ppm: 138.91 (C2), 133.74 (C1), 130.81 (C3), 125.79 (C4), 55.33 (C8), 52.42 (C5), 43.39 (C6), 39.33 (C9), 26.62 (C7). ESI-MS (CH₃CN, m/z): 282.4 (100) [C₁₅H₂₅ClN₃]⁺.

L₁-Br. Under N₂ atmosphere, 6 equivalents of acid (H₂SO₄ 1M, 33 μL, 0.033 mmols) are added dropwise to a stirred solution of complex **1_{Br}** (5.1 mg, 0.011 mmols) in previously deoxygenated CH₃CN (3 mL), causing a color change from purple to colorless in minutes (100% NMR yield). The organic product is extracted in NH₄OH/CH₂Cl₂. The organic phase is dried with MgSO₄ and then dried under vacuum overnight to obtain a yellow oil. ¹H-NMR (CDCl₃, 400MHz) δ, ppm: 7.13 (m, 3H, H^a, H^b), 4.40 (d, J=18.8Hz, 2H, H^c or H^d), 3.57 (d, J=18.8Hz, 2H, H^c or H^d), 2.37 (m, 2H, Hⁱ or H^j), 2.33 (m, 2H, H^e or H^f), 2.16 (m, 2H, H^e or H^f), 1.97 (m, 2H, Hⁱ or H^j), 1.87 (s, 3H, CH₃), 1.52 (m, 4H, H^g, H^h). ¹³C-NMR (CDCl₃, 400MHz) δ, ppm: 140.86 (C2), 130.77 (C3), 126.18 (C4), 125.51 (C1), 55.29 (C8), 54.51 (C5), 42.79 (C6), 39.16 (C9), 26.82 (C7). ESI-MS (CH₃CN, m/z): 326.1(100) [C₁₅H₂₅BrN₃]⁺.

Alternative work-up for L₁-Br. After addition of acid to **1_{Br}** (400.8 mg, 85.14 μmol), 1,10-phenanthroline (150 mg, 160 μmol) was added to the acetonitrile solution, resulting in a color change from colorless to red. The acetonitrile was removed under vacuum, and approx. 100mL CH₂Cl₂ added to the resulting residue. The organic layer was washed with an HCl solution (pH~3) and the layers separated. The aqueous layer was basified (pH~13) and washed with CH₂Cl₂ to yield 240 mg (86 % yield) of **L₁-Br**.

L₁-I. Under N₂ atmosphere 20 equivalents of HPF₆ 15.8 M (15 μL, 0.24 mmols) are added dropwise to a stirred solution of complex **1_I** (6.6 mg, 0.012 mmols) in previously deoxygenated CD₃CN (3 mL) causing a color change from green to pale-yellow. ¹H-NMR spectra of the resultant solution after 1 hour showed 85% yield of coupling product L₁-I(H⁺). ¹H-NMR (CDCl₃, 400MHz) δ, ppm: 7.70 (s, 3H), 4.67 (m, 4H), 3.22 (m, 2H), 3.06 (m, 2H), 2.92 (m, 4H), 2.74 (s, 3H), 1.74 (m, 2H), 1.39 (m, 2H). ESI-MS (CD₃CN, m/z): 374.0(100) [C₁₅H₂₅IN₃]⁺.

L₂-Cl. *Method 1:* Under N₂ atmosphere, 6 equivalents of acid (H₂SO₄ 1 M, 38 μL, 0.038 mmols) are added dropwise to a stirred solution of complex **2_{Cl}** (4.6 mg, 0.013 mmols) in previously deoxygenated CH₃CN (3 mL), causing a color change from red to colorless in minutes. After stirring for 30 minutes, the solution became cloudy and a precipitate appeared quantitatively (no organic products remained in solution, as determined by ¹H-NMR). The solvent is decanted and the precipitate is extracted in NH₄OH/CH₂Cl₂. The organic phase is dried with MgSO₄, filtered and then dried under vacuum overnight to afford a white solid.

Method 2. Under N₂ atmosphere, 3 equivalents of acid (HCl 1M, 32 μL, 0.032 mmols) are added dropwise to a stirred solution of complex [L₂C-Cu^{III}](ClO₄)₂ (5.6 mg, 0.011 mmols) in previously deoxygenated CH₃CN (3 mL), causing a color change from red to colorless in minutes. After stirring for 30 minutes, the solution became cloudy and a precipitate appeared quantitatively (no organic products remained in solution, as determined by ¹H-NMR). The solvent is decanted and the precipitate is extracted in NH₄OH/CH₂Cl₂. The organic phase is dried with MgSO₄ and then dried under vacuum overnight to yield a white solid.

¹H-NMR (CDCl₃, 400MHz) δ, ppm: 7.14 (m, 3H, H^a, H^b), 4.41 (d, J=14Hz, 2H, H^c or H^d), 3.55 (d, J=14Hz, 2H, H^c or H^d), 2.6 (m, 4H, Hⁱ, H^j), 2.4 (m, 2H, H^e or H^f), 2.15 (td, J=11.6Hz, J=2.8Hz, 2H, H^e or H^f), 1.7 (m, 2H, H^g or H^h), 1.65 (m, 2H, H^g or H^h). ¹³C-NMR (CDCl₃, 400MHz) δ, ppm: 139.02 (C2), 133.10 (C1), 131.17 (C3), 125.61 (C4), 52.32 (C8), 45.66 (C5), 41.46 (C6), 28.46 (C7). ESI-MS (CH₃CN, m/z): 268.2(100) [C₁₄H₂₃ClN₃]⁺.

L₂-Br. Under N₂ atmosphere, 6 equivalents of acid (H₂SO₄ 1M, 72 μL, 0.072 mmols) are added dropwise to a stirred solution of complex **2_{Br}** (10.9 mg, 0.024 mmols) in previously deoxygenated CH₃CN (3 mL), causing a color change from purple to colorless in hours. After stirring overnight, the solution became cloudy and a precipitate appeared (no organic products remained in solution, as determined by ¹H-NMR). The solvent is decanted and the precipitate is extracted in NH₄OH/CH₂Cl₂. The organic phase is dried with MgSO₄ and then dried under vacuum overnight to yield a white solid. ¹H-NMR (CDCl₃, 400MHz) δ, ppm: 7.13 (m, 3H, H^a, H^b), 4.37 (d, J=14Hz, 2H, H^c or H^d), 3.57 (d, J=14Hz, 2H, H^c or H^d), 2.61 (t, J=12Hz, 2H, Hⁱ or H^j), 2.53 (m, 2H, Hⁱ or H^j), 2.40 (m, 2H, H^e or H^f), 2.09 (td, J=11.6Hz, J=2.8Hz, 2H, H^e or H^f), 1.7 (m, 2H, H^g or H^h), 1.59 (m, 2H, H^g or H^h). ¹³C-NMR (CDCl₃, 400MHz) δ, ppm: 140.67 (C2), 131.30 (C3), 126.15 (C4), 124.80 (C1), 54.20 (C5), 45.55 (C8), 41.08 (C6), 28.45 (C7). ESI-MS (CH₃CN, m/z): 312.0(100) [C₁₄H₂₃BrN₃]⁺.

1.5. Crystallographic characterization of aryl-Cu^{III}-halide complexes

Crystals of complexes **1_I**, **2_{Cl}** and **2_I** were grown from slow diffusion of ethyl ether in a CH₃CN solution of the compound and crystals of complexes **1_{Cl}** and **1_{Br}** were grown from slow diffusion of ethyl ether in a DMF solution of the compound. All of them were used for room temperature (300(2) K) X-ray structure determination. The

measurement was carried out on a *BRUKER SMART APEX CCD* diffractometer using graphite-monochromated Mo $K\alpha$ radiation ($(\lambda = 0.71073 \text{ \AA})$ from an x-Ray Tube. Crystal data is found in Tables S4-S5. Programs used: data collection, Smart version 5.631 (Bruker AXS 1997-02); data reduction, Saint + version 6.36A (Bruker AXS 2001); absorption correction, SADABS version 2.10 (Bruker AXS 2001). Structure solution and refinement was done using SHELXTL Version 6.14 (Bruker AXS 2000-2003). The structure was solved by direct methods and refined by full-matrix least-squares methods on F². The non-hydrogen atoms were refined anisotropically. The H-atoms were placed in geometrically optimized positions and forced to ride on the atom to which they are attached, except N-H hydrogens which were located in the difference Fourier map and refined without constraints.

Crystal data for **1_{Cl}**, **1_{Br}**, **1_I**, **2_{Cl}** and **2_I** have been deposited as CCDC references 735508-735512, respectively, which contain the supplementary crystallographic data for each compound. These data can be obtained free of charge from CCDC via www.ccdc.cam.ac.uk/data_request/cif.

1.6. General Procedure for Monitoring Catalytic Coupling of **L₁-Br** with Pyridone by NMR Spectroscopy

In an inert-atmosphere glove box, stock solutions of **L₁-Br**/trimethoxybenzene (9.6/14.9 mM) and pyridone/Cu(CH₃CN)₄PF₆ (151/4.4 mM) were prepared in CD₃CN (5 mL each). The **L₁-Br**/trimethoxybenzene stock solution (700 μ L) was added to an NMR tube and capped with a septum. To initiate the reaction, 50 μ L of the pyridone/[Cu^I(CH₃CN)₄]PF₆ solution was added to the NMR tube, and the tube was placed in the NMR probe, pre-cooled to 288 K. The dead time between addition and data acquisition was 2 min. The final concentrations were as follows: [L₁-Br] = 8.9 mM, [pyridone] = 10.1 mM, and [Cu^I(CH₃CN)₄]PF₆ = 0.3 mM. Full-scale NMR spectra acquired during the catalytic timecourse are shown in Figure S53. The same stock solutions were used to acquire the UV-Vis timecourse data. The **L₁-Br**/trimethoxybenzene stock solution (1.05 mL) was added to a 1-cm pathlength quartz cuvette and the solution was cooled to 288 K in the sample holder. The reaction was initiated by addition of the pyridone/[Cu^I(CH₃CN)₄]PF₆ solution (75 μ L).

2. Supplementary Figures

Figure S1. ^1H -NMR spectrum of complex $\mathbf{1}_{\text{Cl}}$ in DMSO-d_6 , 500MHz, at 298K.

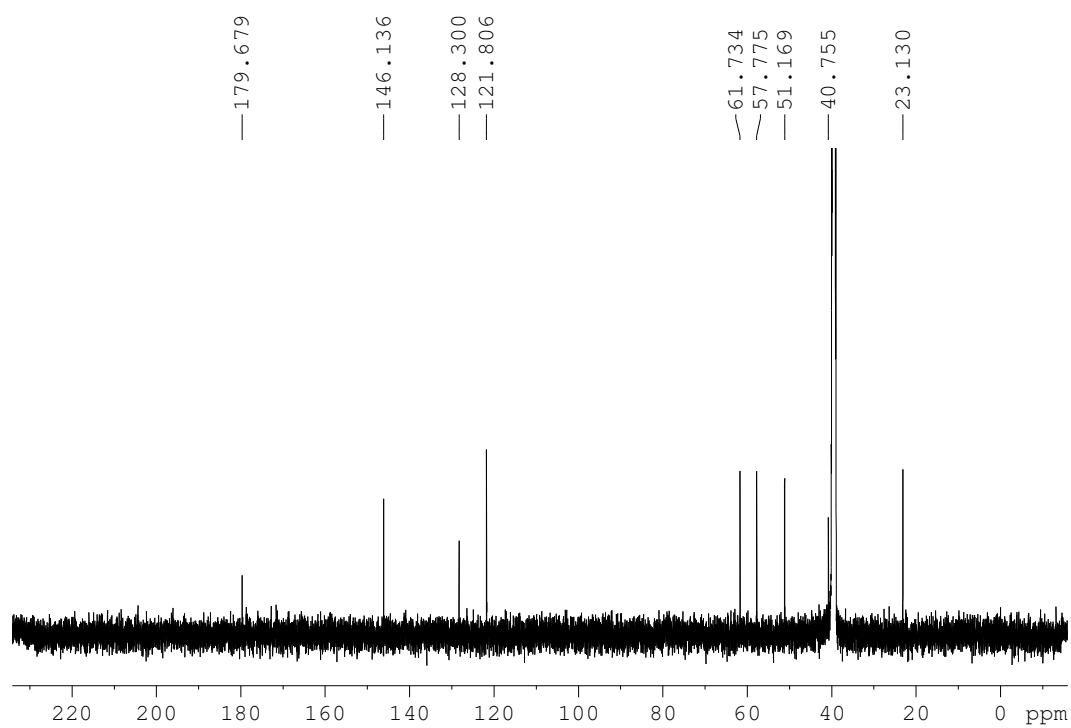
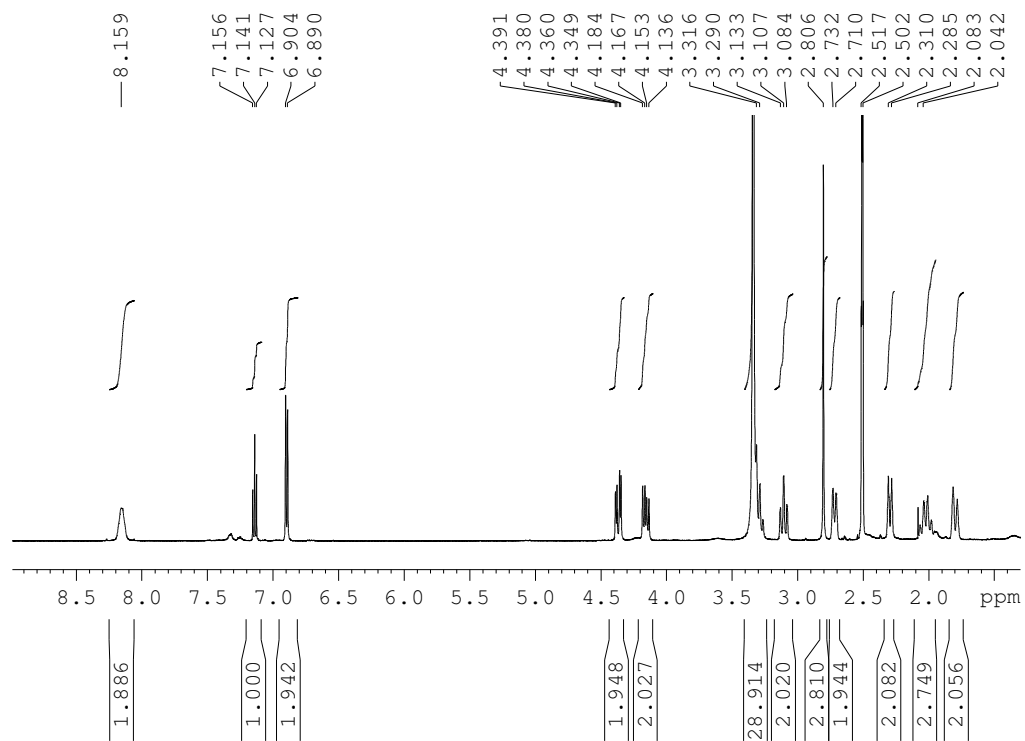


Figure S3. COSY spectrum of complex **1Cl** in DMSO-d₆, 500MHz, at 298K.

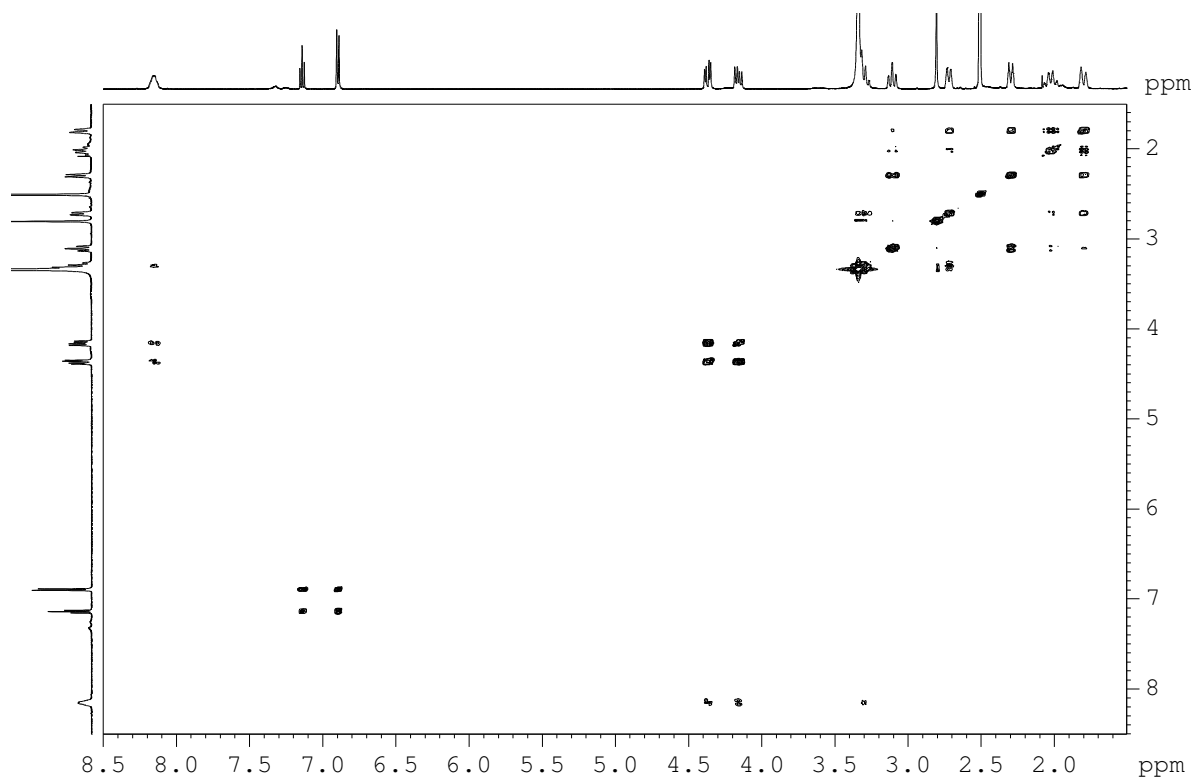


Figure S4. NOESY spectrum of complex **1Cl** in DMSO-d₆, 500MHz, at 298K.

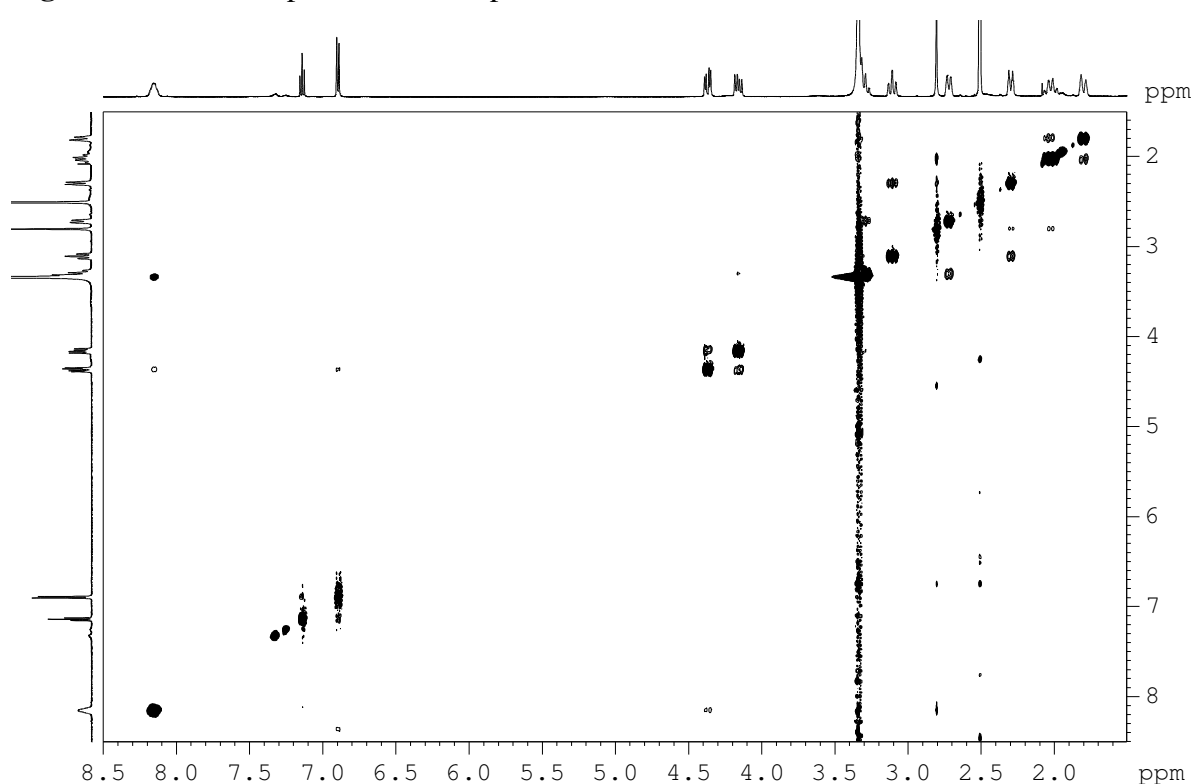


Figure S5. HSQC spectrum of complex **1Cl** in DMSO-d₆, 500MHz, at 298K.

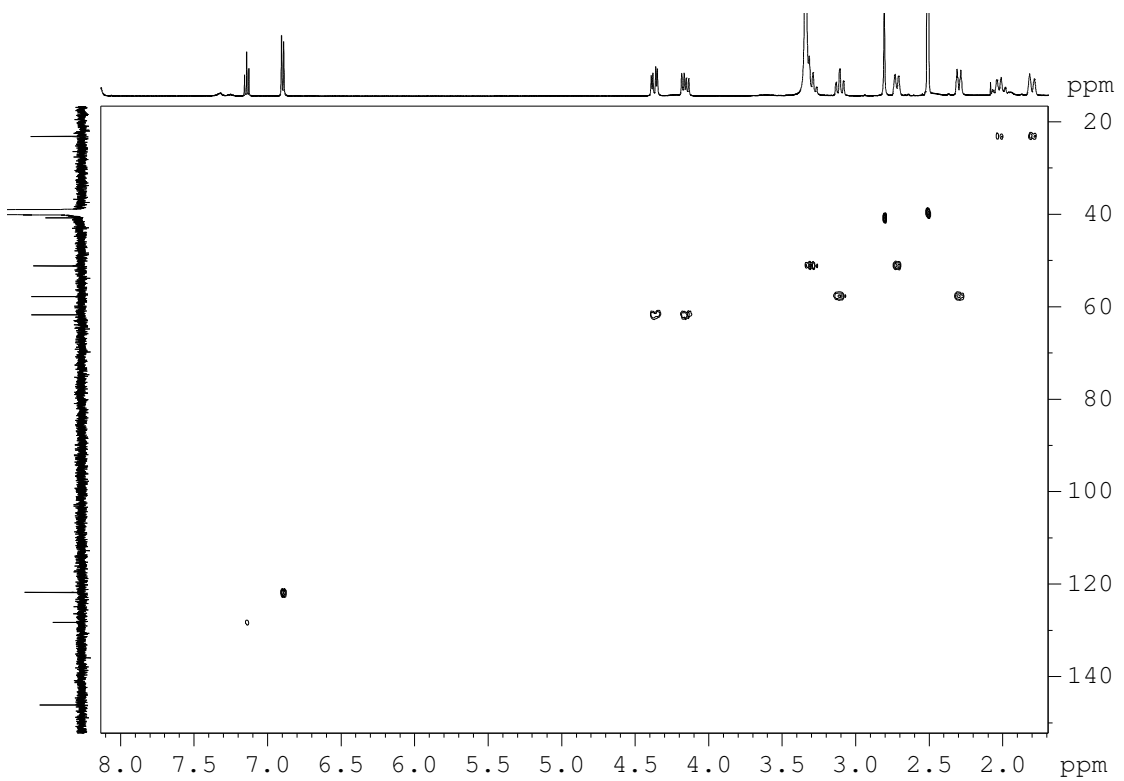


Figure S6. HMBC spectrum of complex **1Cl** in DMSO-d₆, 500MHz, at 298K.

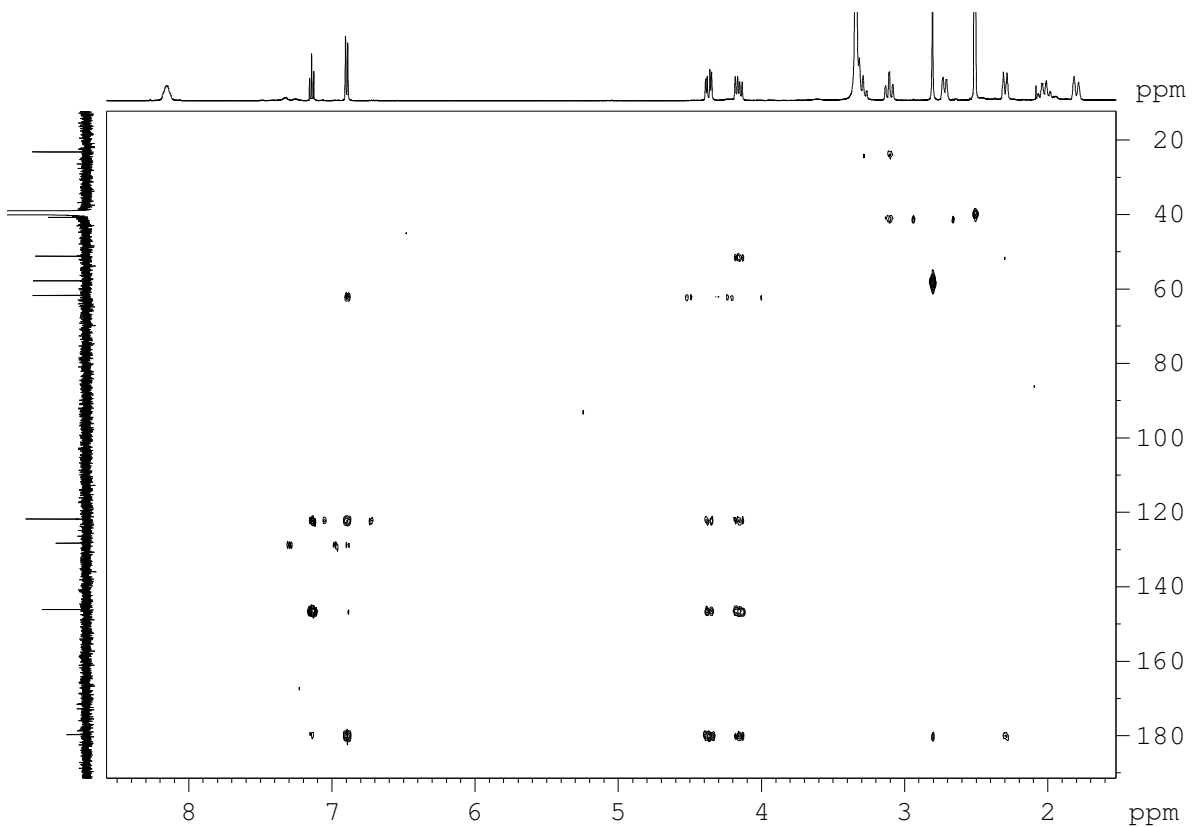


Figure S7. ^1H -NMR spectrum of complex $\mathbf{1}_{\text{Br}}$ in DMSO-d_6 , 400MHz, at 298K.

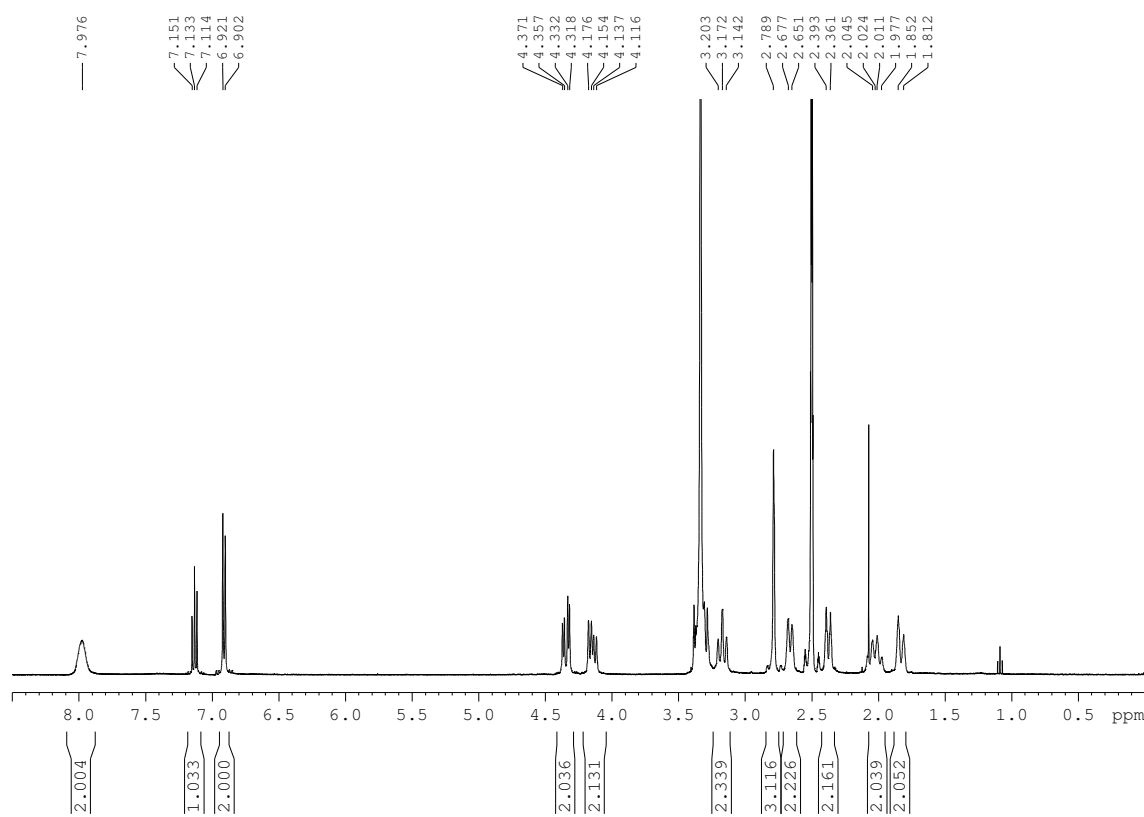


Figure S8. ^{13}C -NMR spectrum of complex $\mathbf{1}_{\text{Br}}$ in DMSO-d_6 , 400MHz, at 298K.

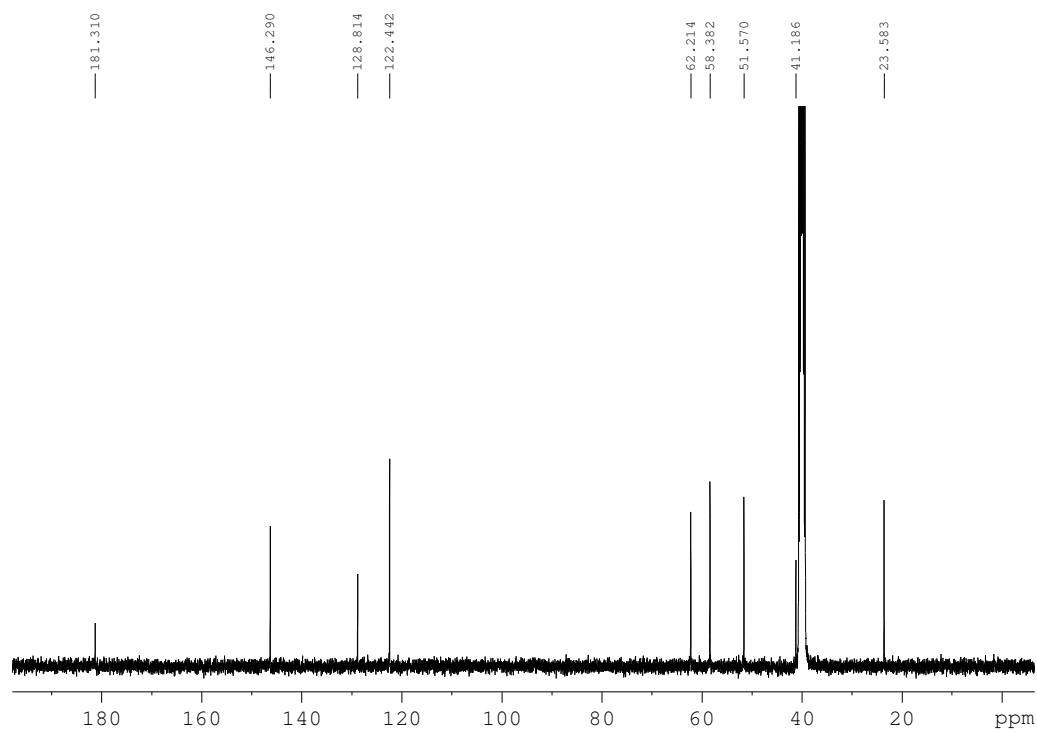


Figure S9. HSQC spectrum of complex **1_{Br}** in DMSO-d₆, 400MHz, at 298K.

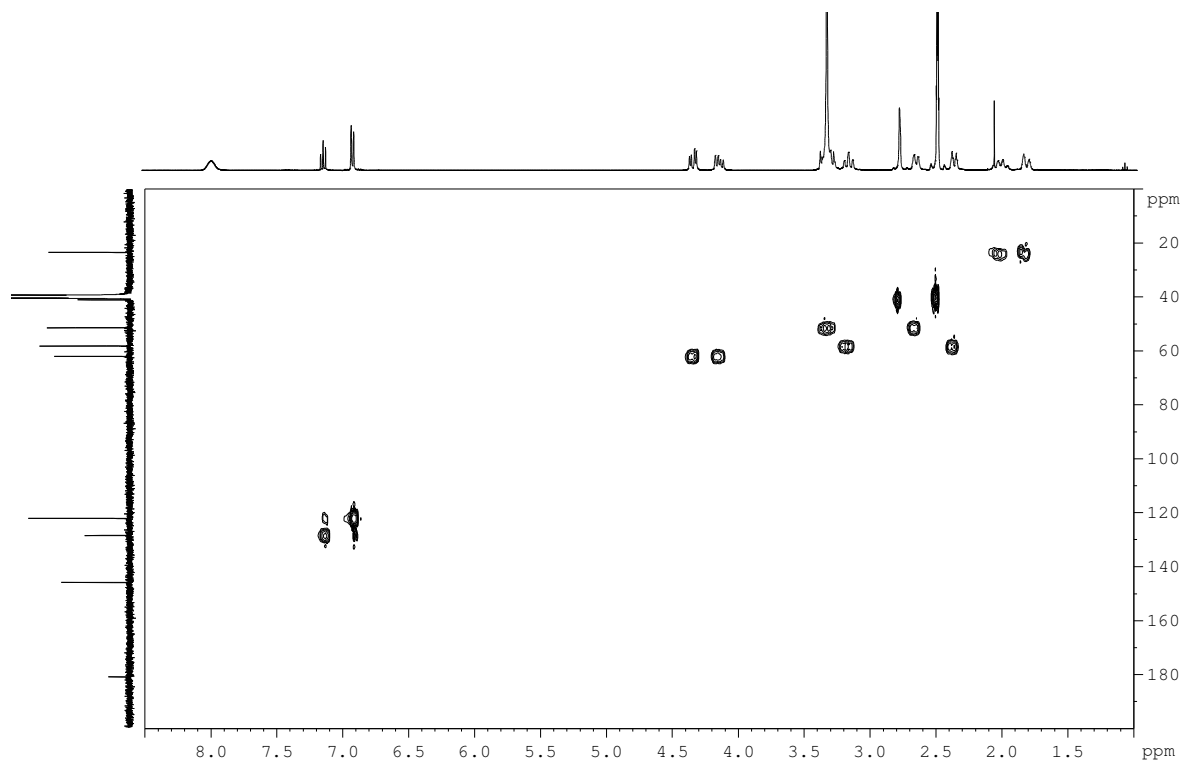


Figure S10. ¹H-NMR spectrum of complex **1_I** in CD₃CN, 300MHz, at 298K.

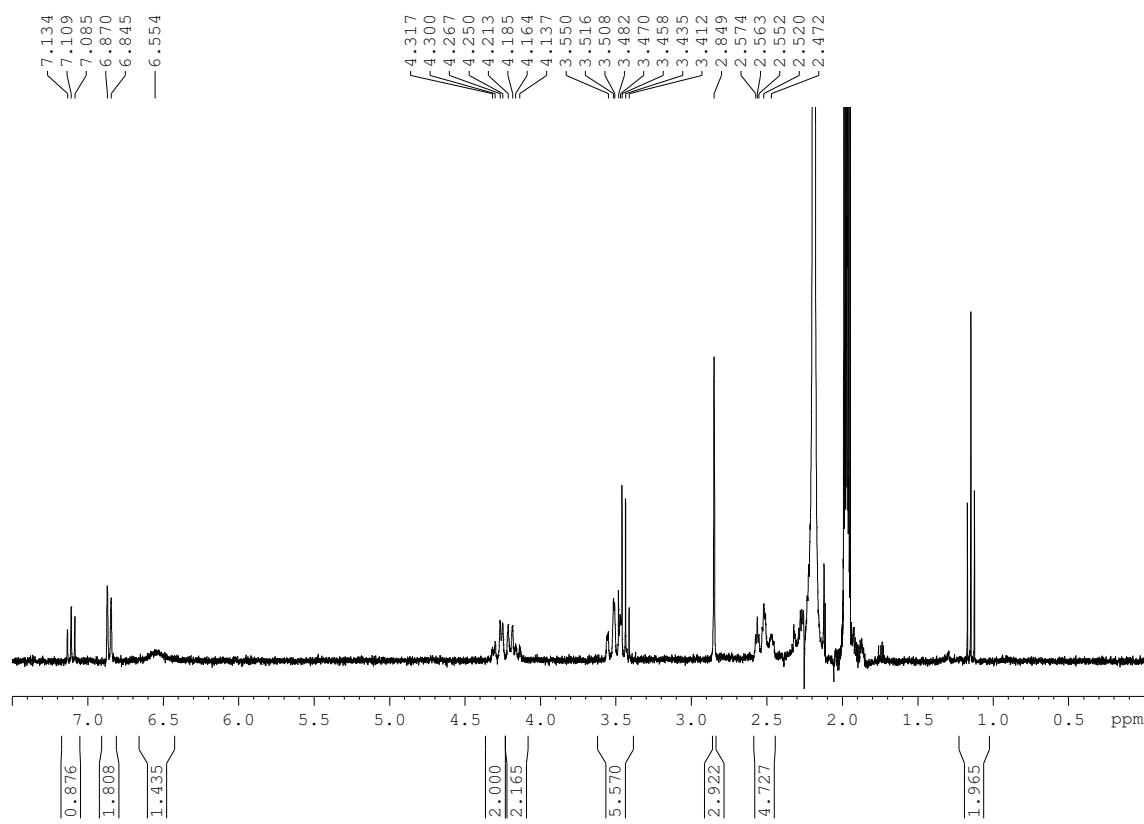


Figure S11. ^{13}C -NMR spectrum of complex **1_I** in CD_3CN , 300MHz, at 298K.

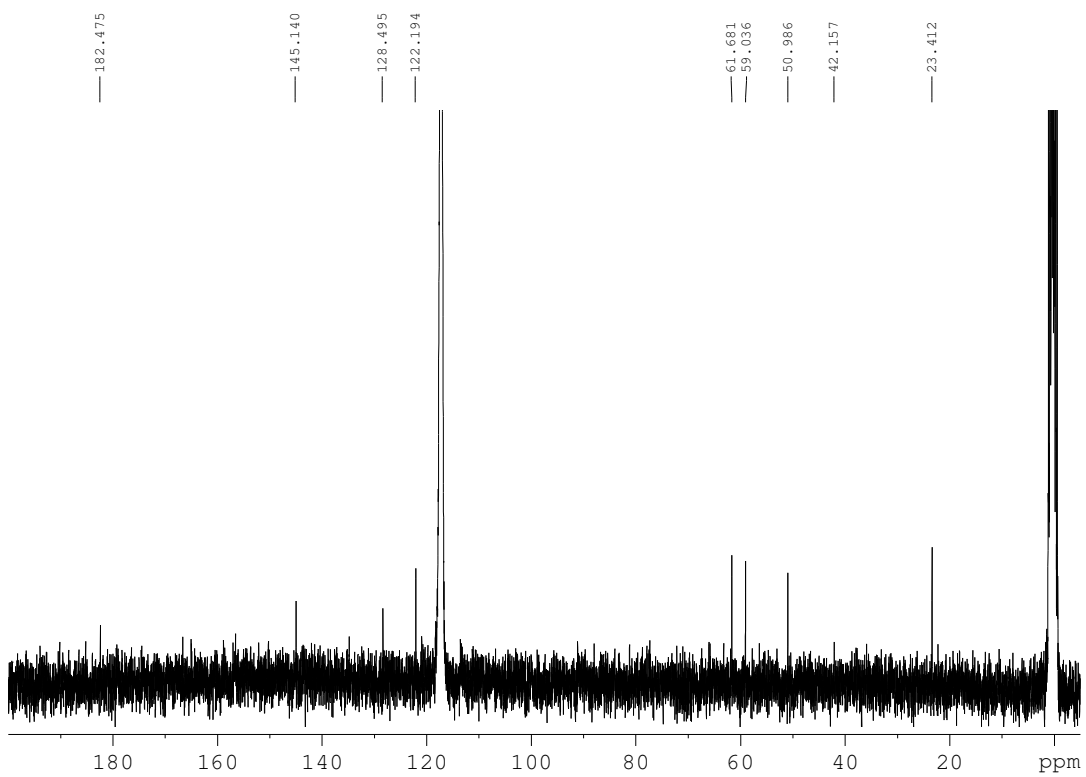


Figure S12. HSQC spectrum of complex **1_I** in CD_3CN , 300MHz, at 298K.

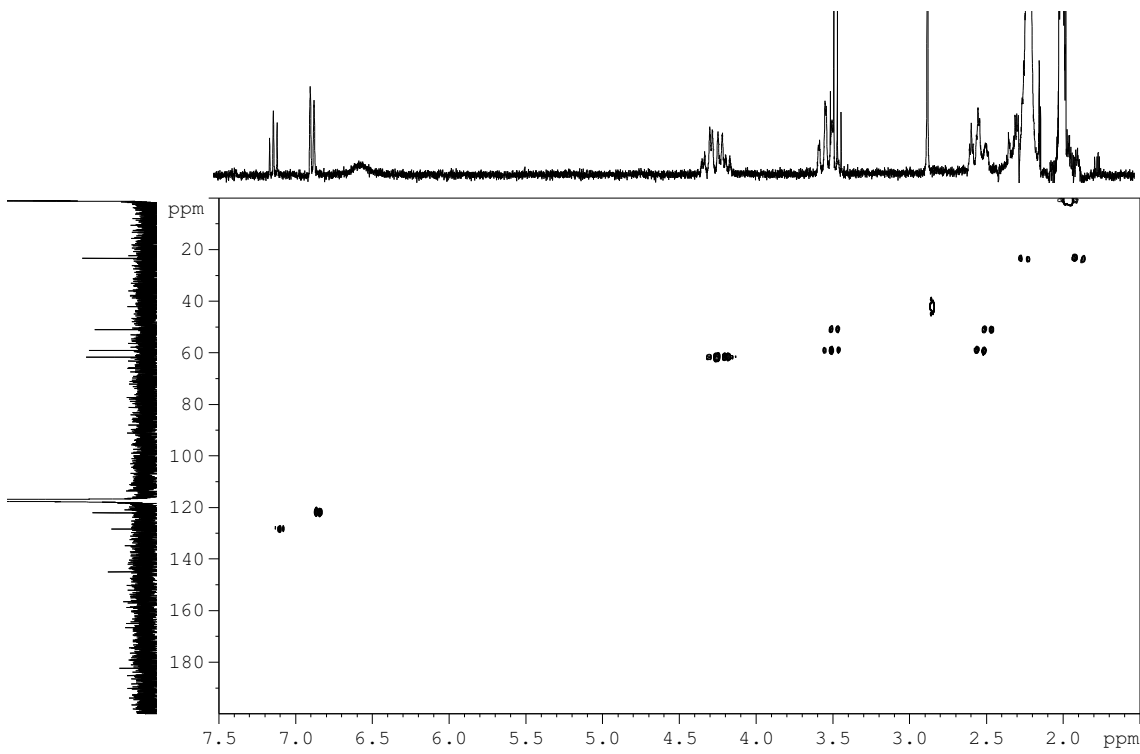


Figure S13. ^1H -NMR spectrum of complex $\mathbf{2}_{\text{Cl}}$ in DMSO-d_6 , 500MHz, at 298K.

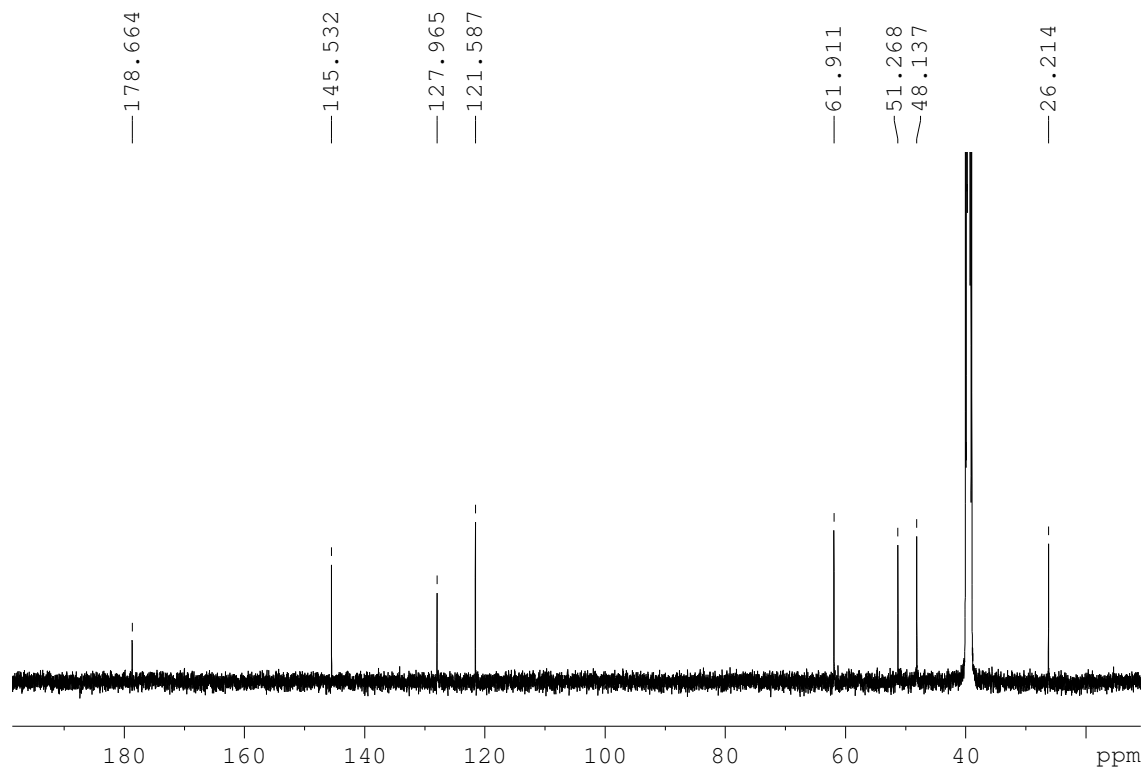
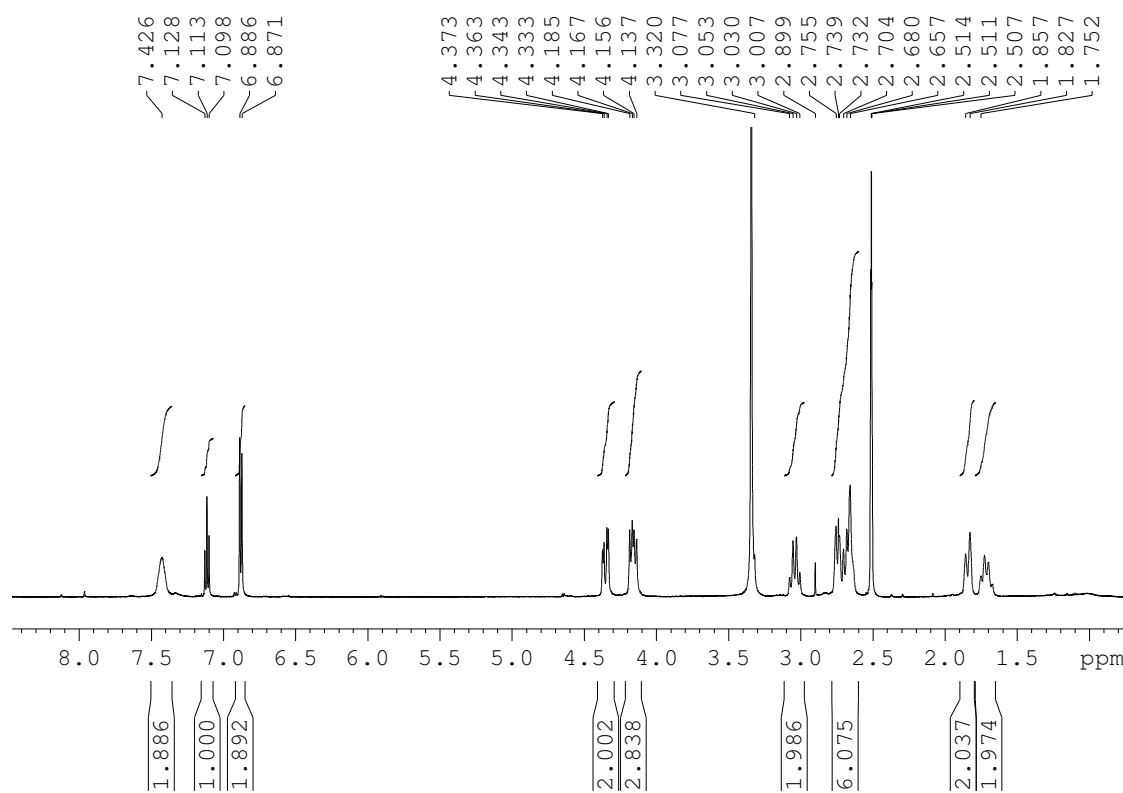


Figure S15. COSY spectrum of complex **2Cl** in DMSO-d₆, 500MHz, at 298K.

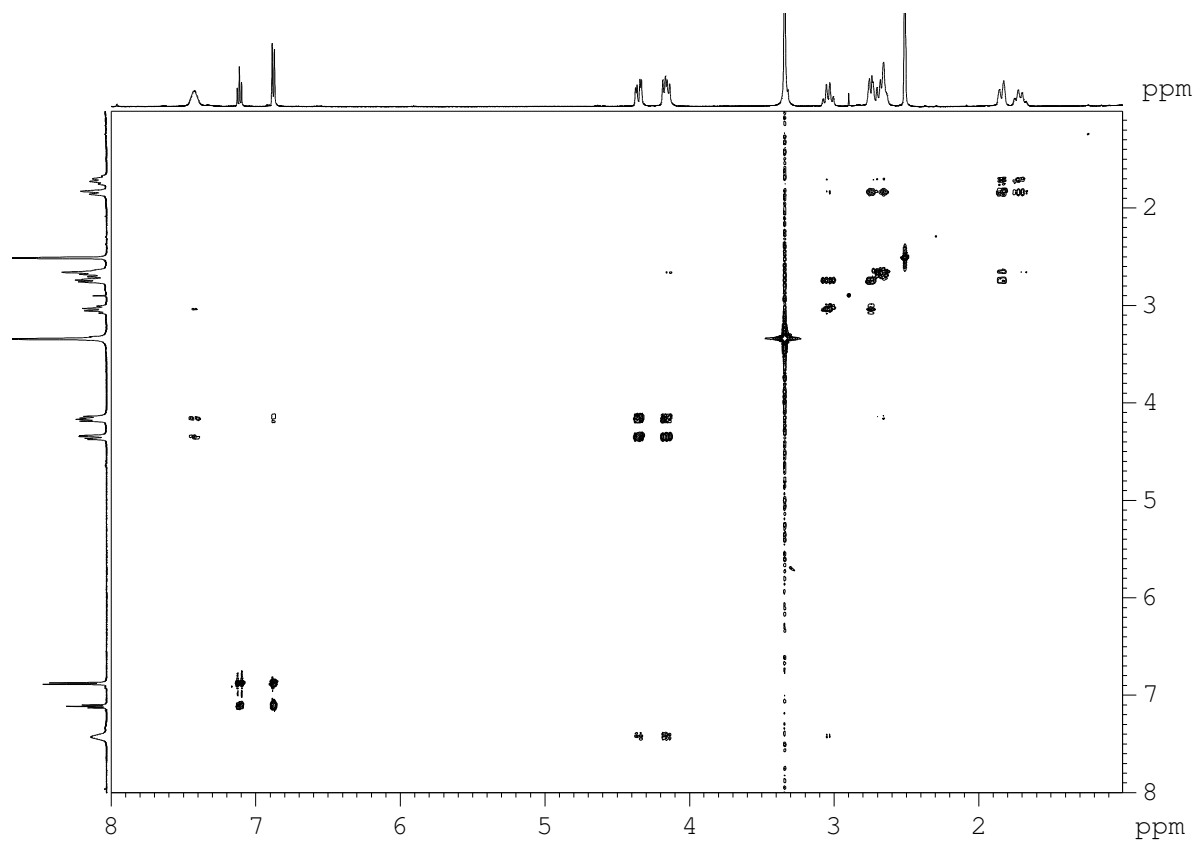


Figure S16. NOESY spectrum of complex **2Cl** in DMSO-d₆, 500MHz, at 298K.

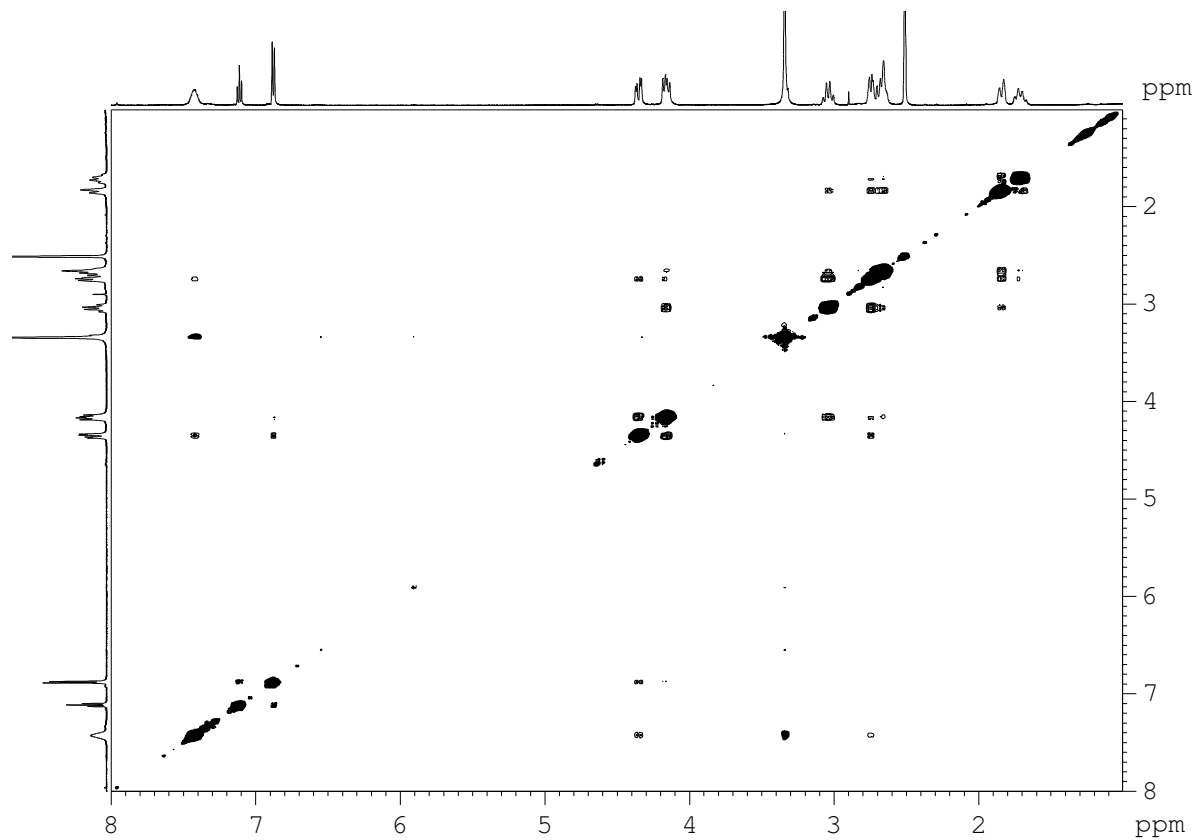


Figure S17. HSQC spectrum of complex **2Cl** in DMSO-d₆, 500MHz, at 298K.

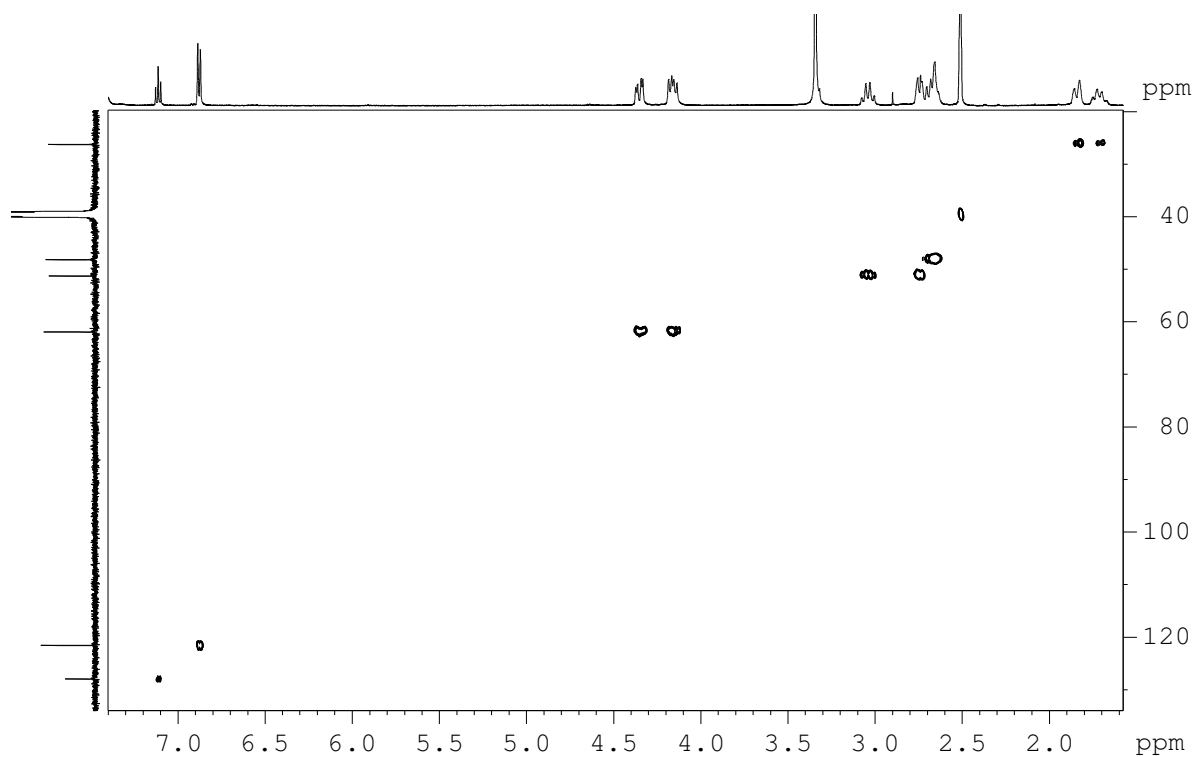


Figure S18. HMBC spectrum of complex **2Cl** in DMSO-d₆, 500MHz, at 298K.

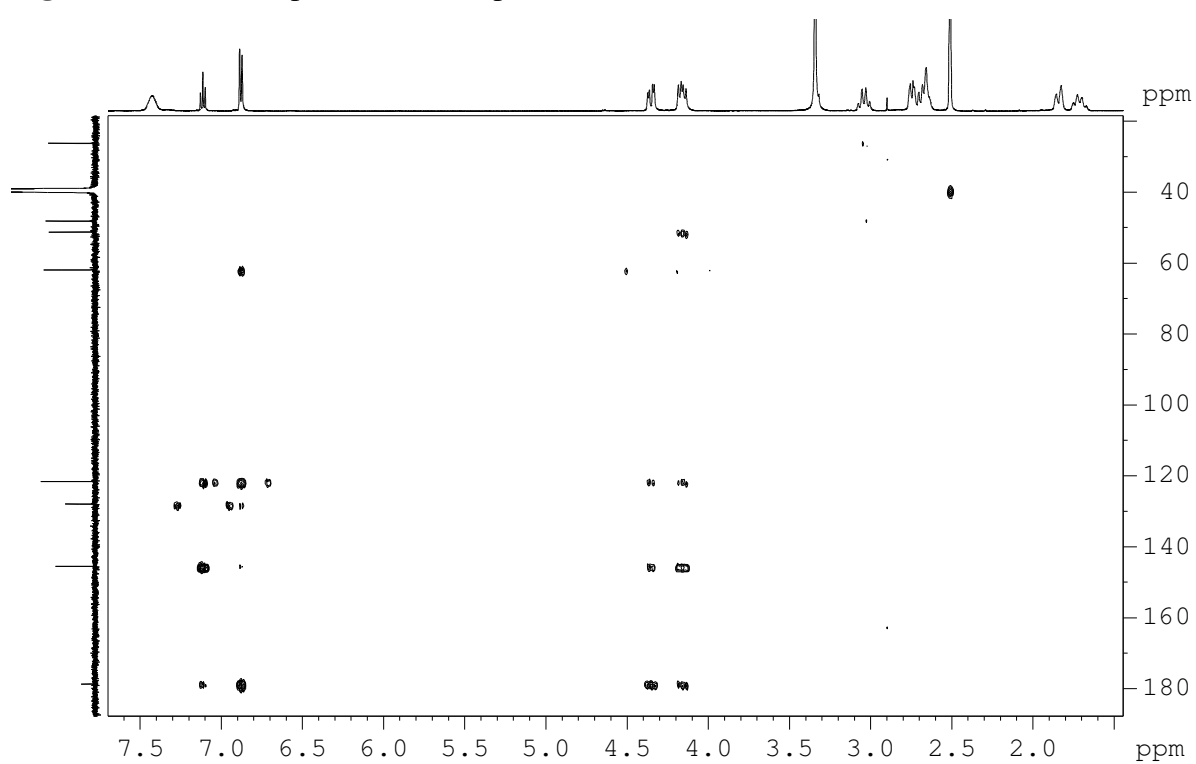


Figure S19. ^1H -NMR spectrum of complex $\mathbf{2}_{\text{Br}}$ in DMSO-d_6 , 400MHz, at 298K.

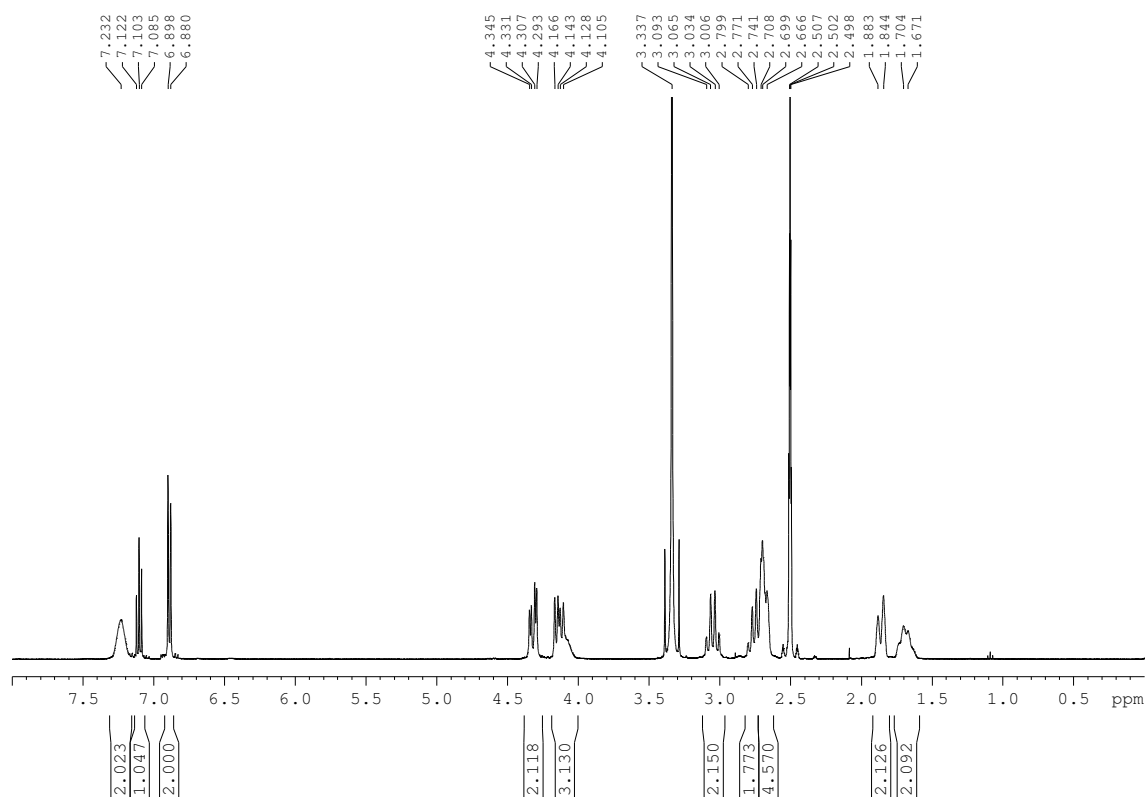


Figure S20. ^{13}C -NMR spectrum of complex $\mathbf{2}_{\text{Br}}$ in DMSO-d_6 , 400MHz, at 298K.

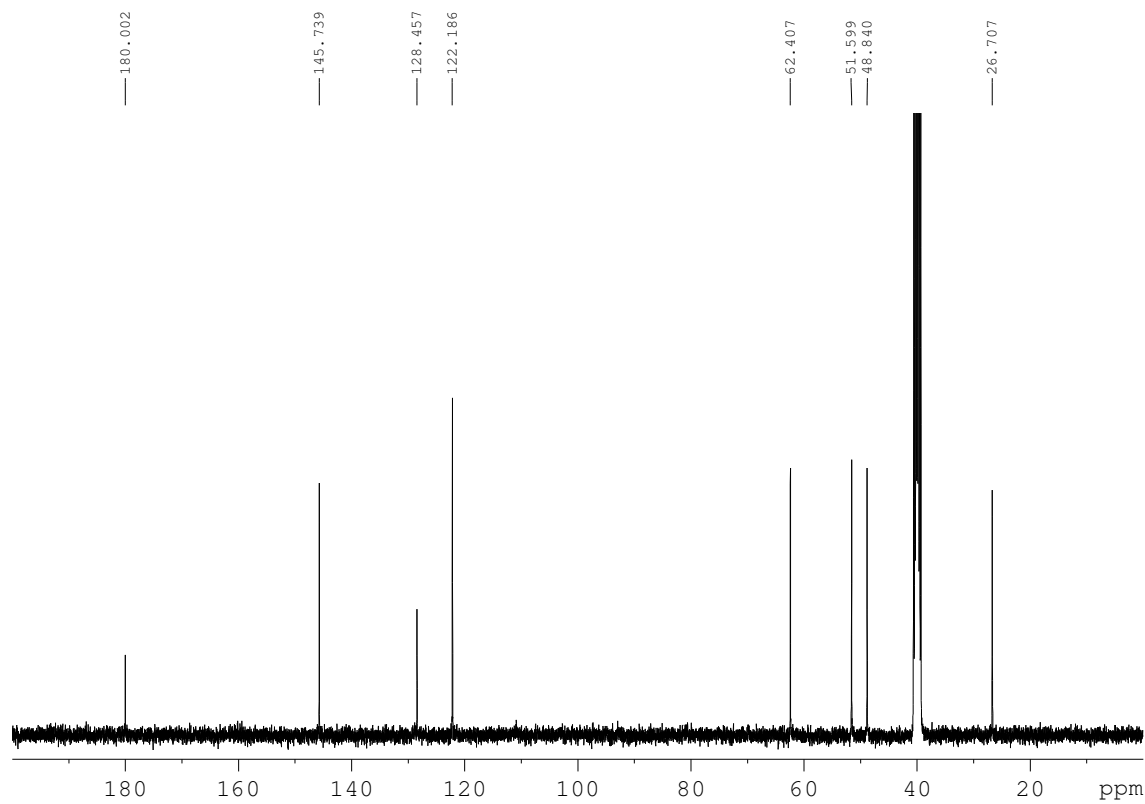


Figure S21. HSQC spectrum of complex **2_{Br}** in DMSO-d₆, 400MHz, at 298K.

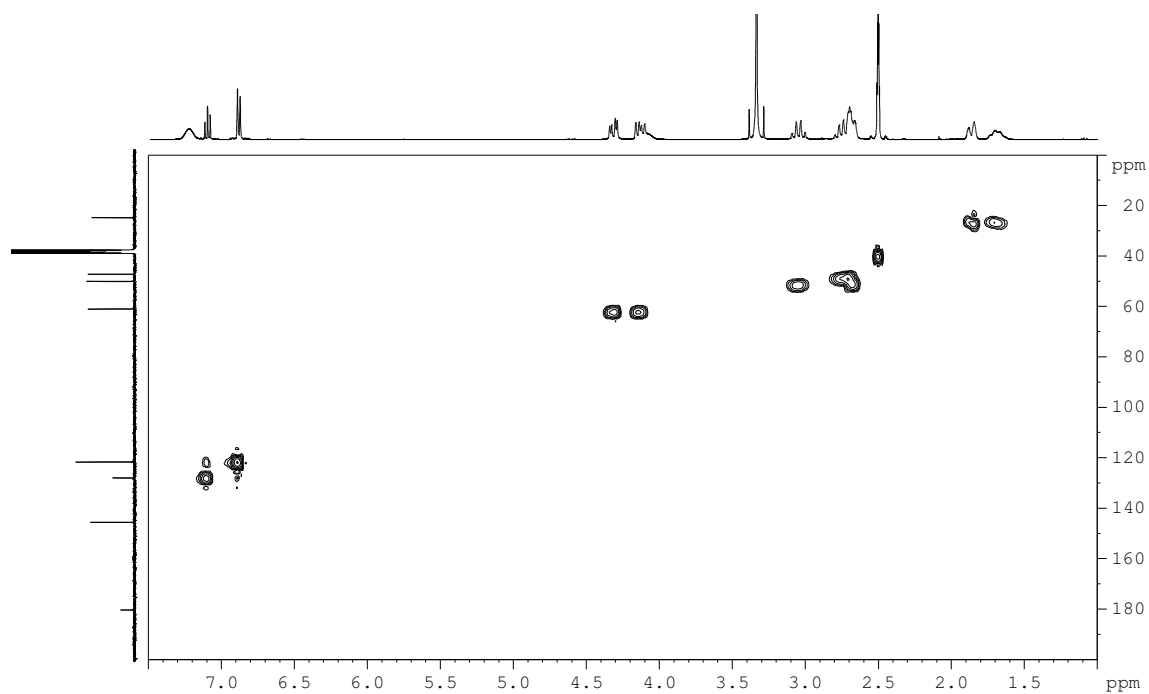


Figure S22. ¹H-NMR spectrum of complex **2_I** in CD₃CN, 400MHz, at 298K.

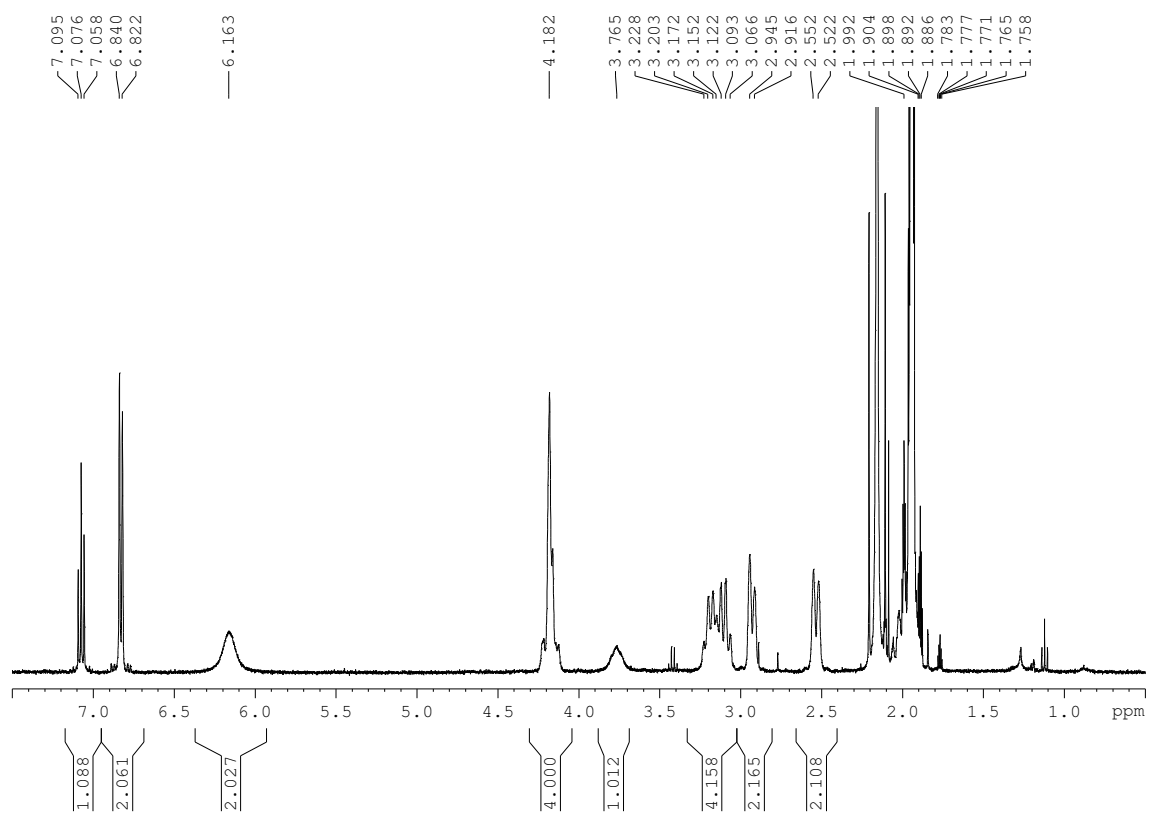


Figure S23. ^{13}C -NMR spectrum of complex **2_I** in CD_3CN , 400MHz, at 298K.

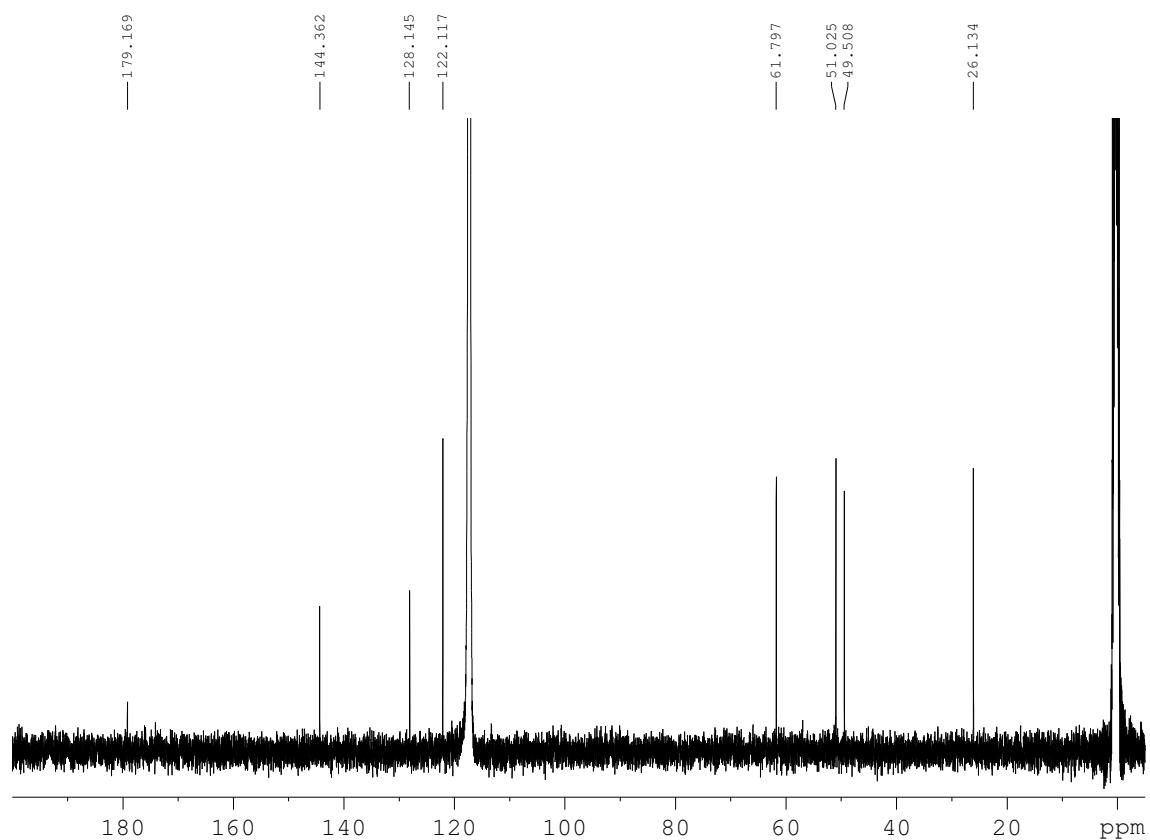


Figure S24. HSQC spectrum of complex **2_I** in CD_3CN , 400MHz, at 298K.

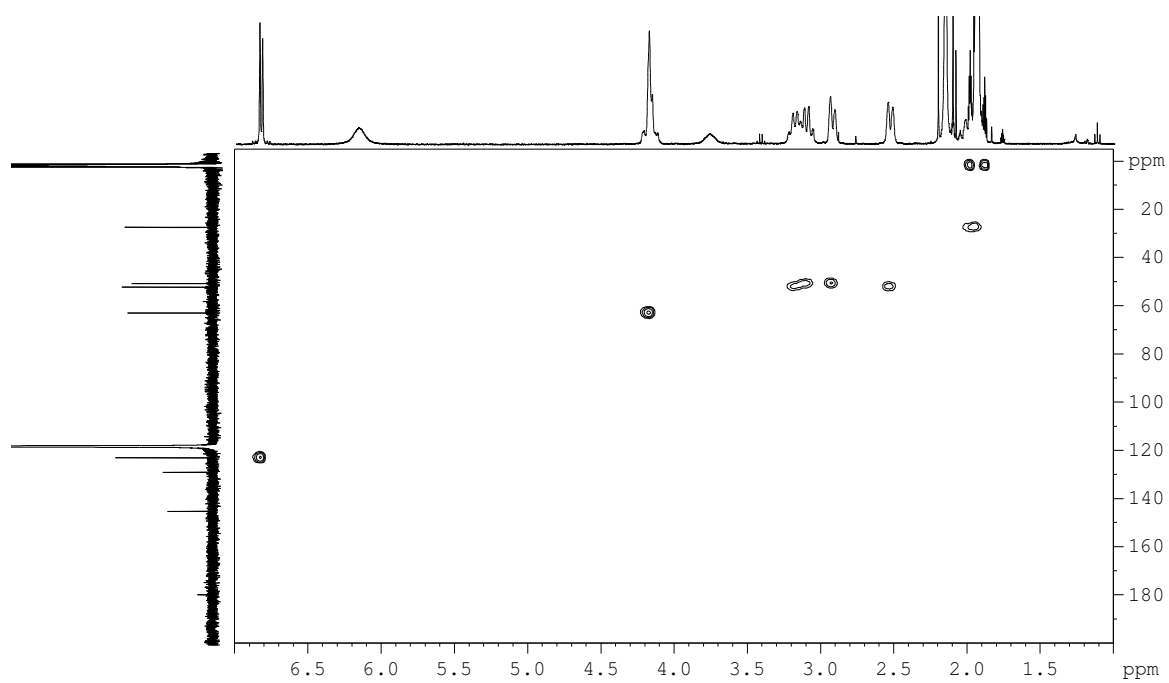


Figure S25. UV-visible spectra for aryl-Cu^{III}-halide complexes $\mathbf{1}_X\text{-}\mathbf{2}_X$ ($X=\text{Cl}, \text{Br}, \text{I}$) complex concentration 0.8 mM in CH₃CN at 298 K.

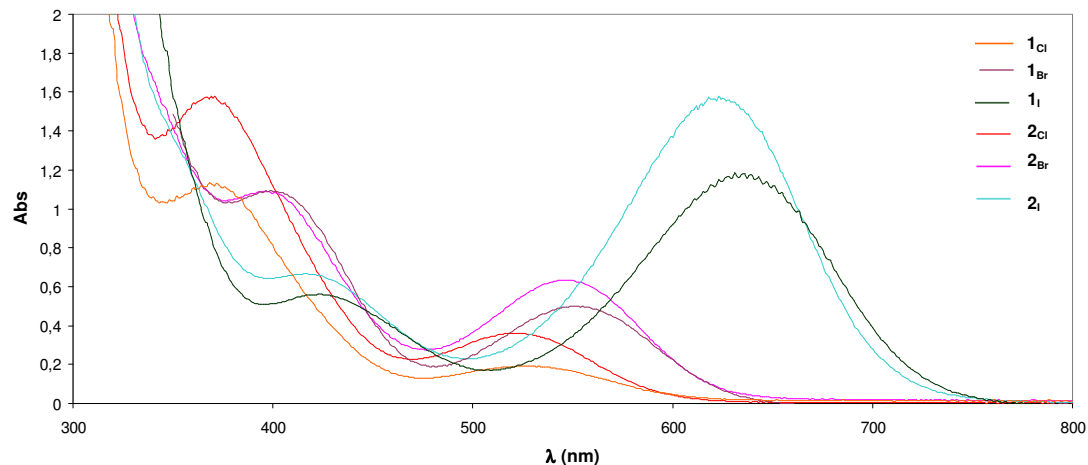


Figure S26. Cyclic voltammetry of aryl-Cu^{III}-halide complexes, $[\text{L}_i\text{C-Cu}^{\text{III}}\text{-X}] = 1 \text{ mM}$, scan rate = 0.2 V/s, TBAP 0.1M, CH₃CN, 263 K, using SSCE as the reference electrode and Fc/Fc⁺ as internal reference.

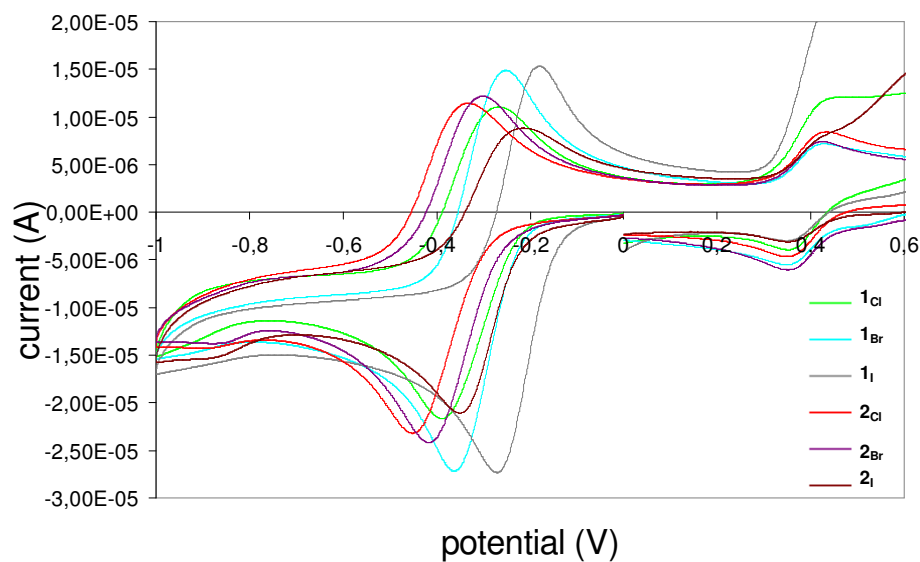


Figure S27. X-ray crystal structure of complex **2_I**. Hydrogen atoms have been omitted for clarity. Selected bond lengths [Å]: Cu-C1 1.911(7), Cu-I1 2.8122(13), Cu-N1 1.997(7), Cu-N2 1.996(6), Cu-N3 1.988(7). See crystal data in Tables 4 and 5 (CCDC code: 735512).

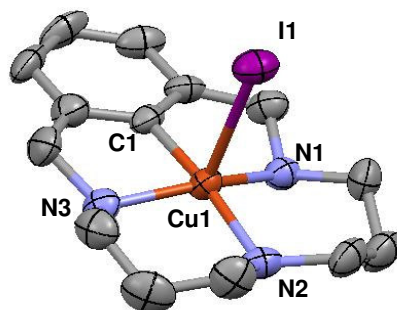


Figure S28. ¹H-NMR spectra of mixture crude of reductive elimination reaction products of complex **1_{Cl}** using 2 equiv. of CF₃SO₃H in CD₃CN, 400 MHz at 298 K. Quantitative formation of protonated coupling product **L₁-Cl(H⁺)** is obtained.

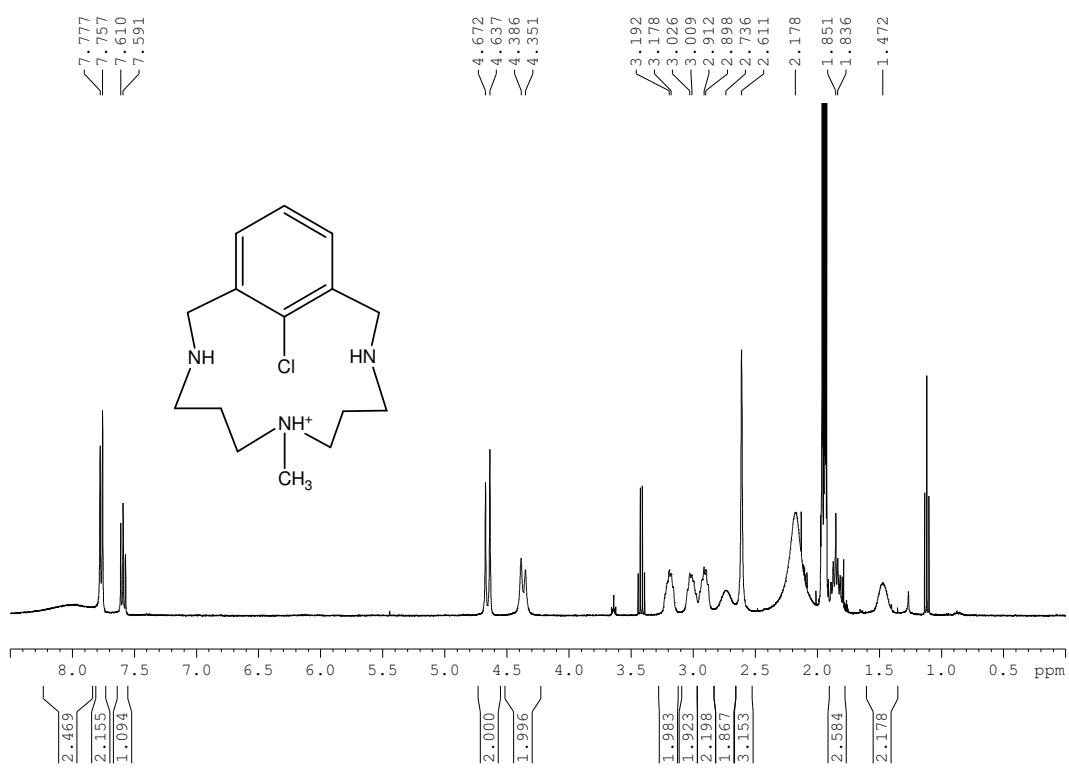


Figure S29. ^1H -NMR spectrum **L₁-Cl** in CHCl_3 , 400MHz, at 298K.

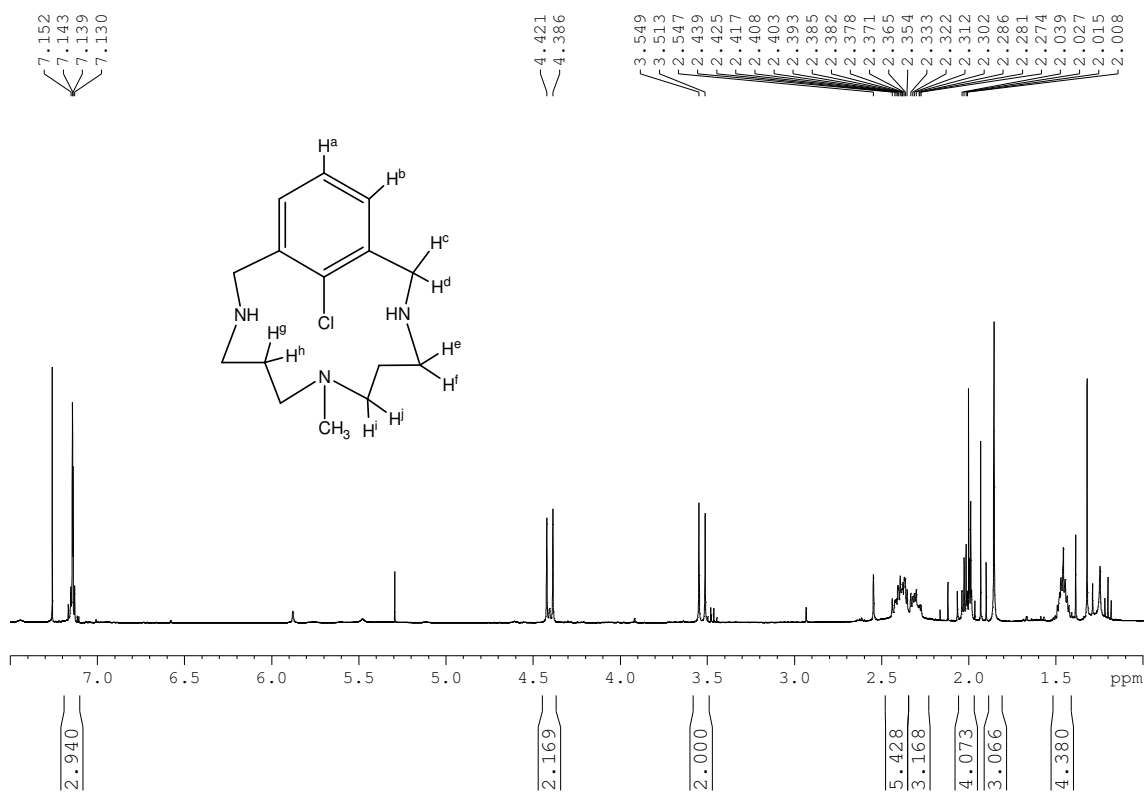


Figure S30. HSQC spectrum L₁-Cl in CHCl₃, 400MHz, at 298K.

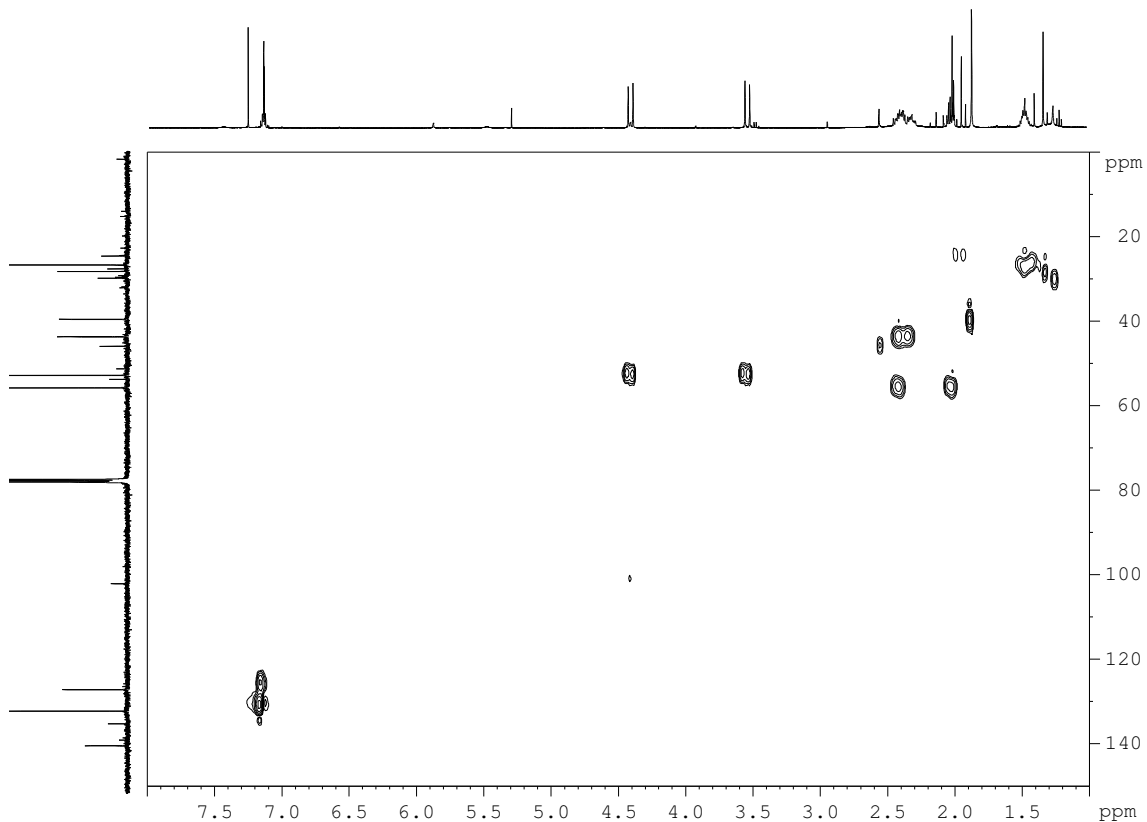


Figure S31. ^{13}C -NMR spectrum of **L₁-Cl** in CHCl_3 , 400MHz, at 298K.

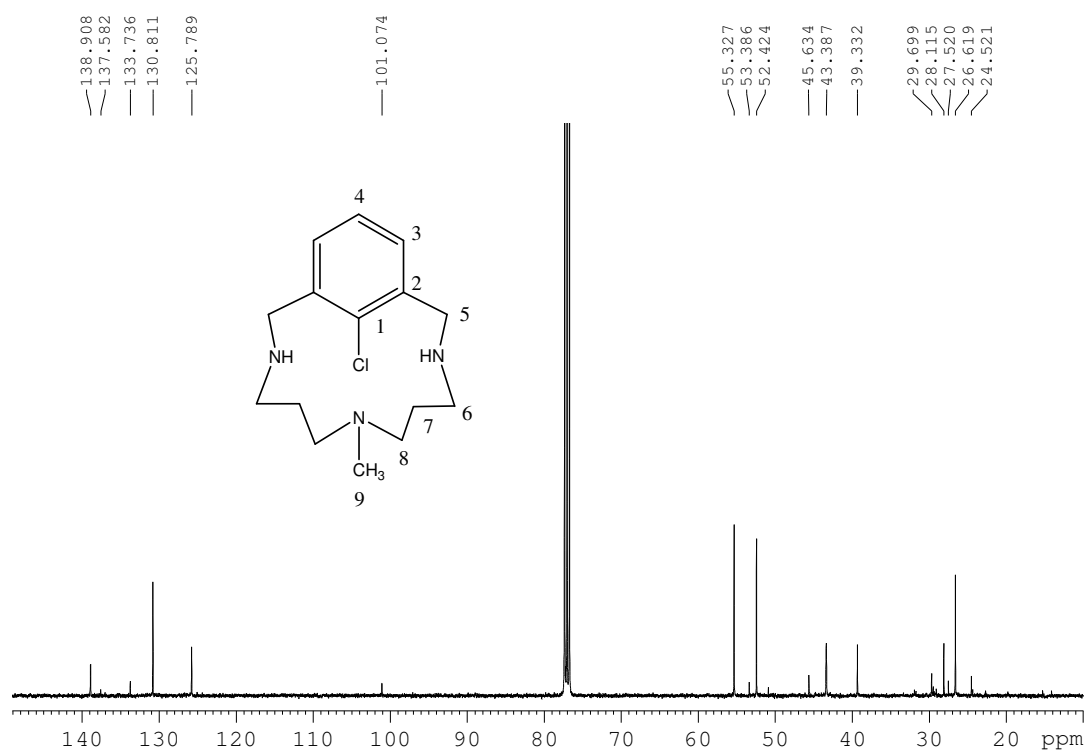


Figure S32. ^1H -NMR spectra of mixture crude of reductive elimination reaction of complex **1_{Br}** using 2 equiv. of $\text{CF}_3\text{SO}_3\text{H}$ in CD_3CN , 400 MHz at 298 K. Quantitative formation of protonated coupling product **L₁-Br(H⁺)** is obtained.

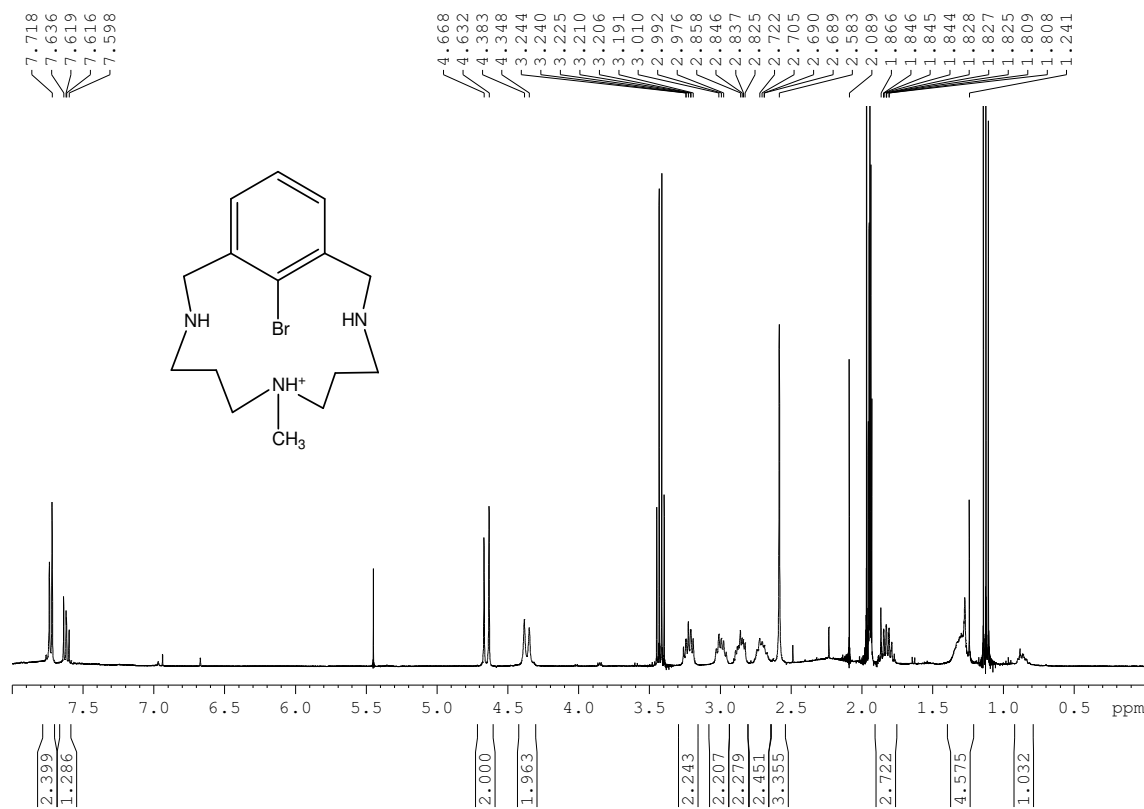


Figure S33. ^1H -NMR spectrum of **L₁-Br** in CHCl_3 , 400MHz, at 298 K.

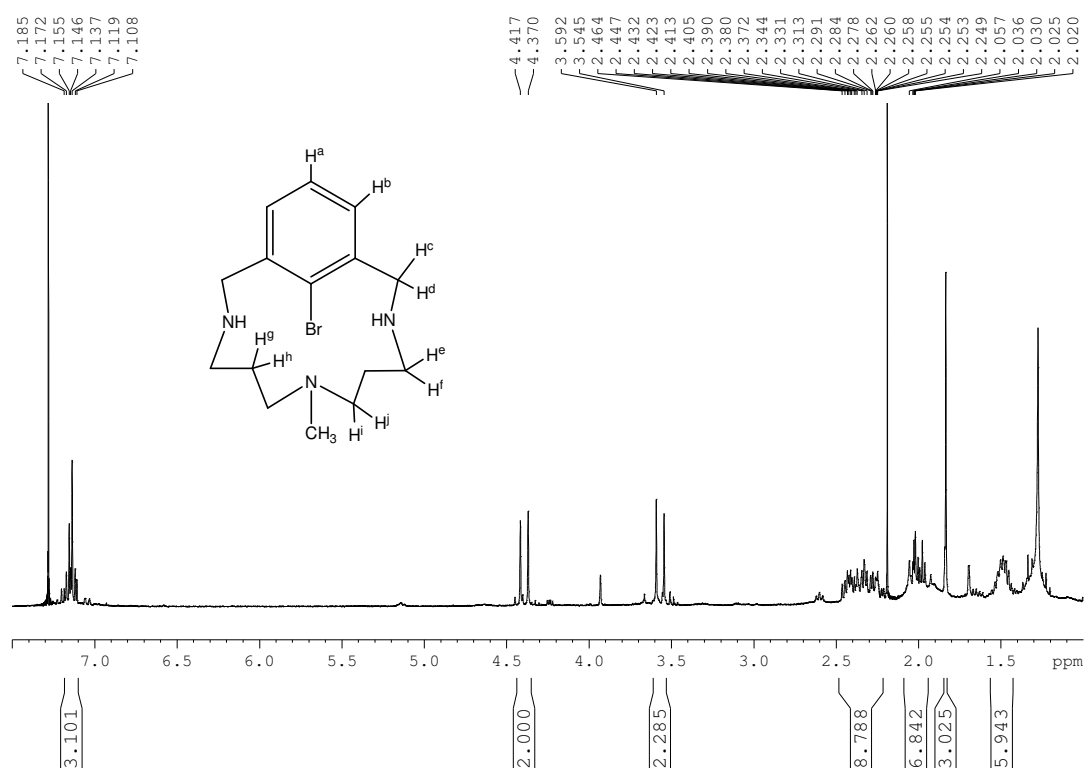


Figure S34. ^{13}C -NMR spectrum of **L₁-Br** in CHCl_3 , 400MHz, at 298K.

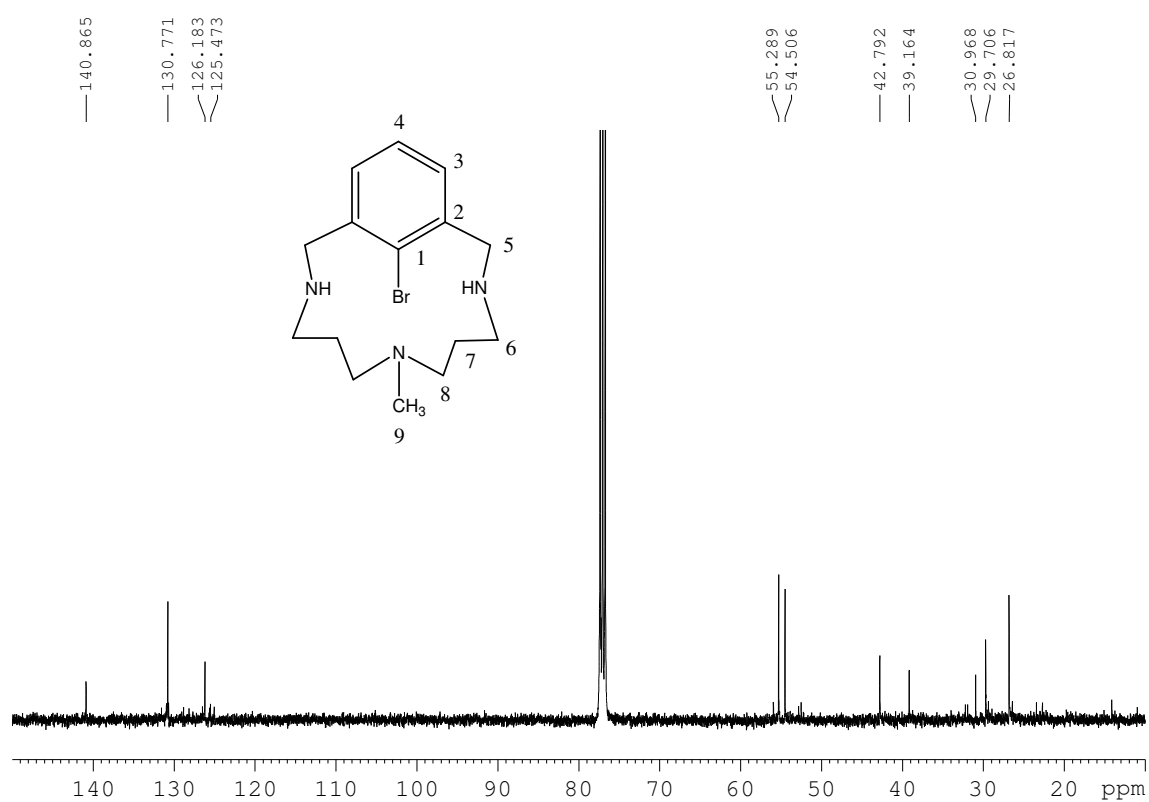


Figure S35. HSQC spectrum L₁-Br in CHCl₃, 400MHz, at 298K.

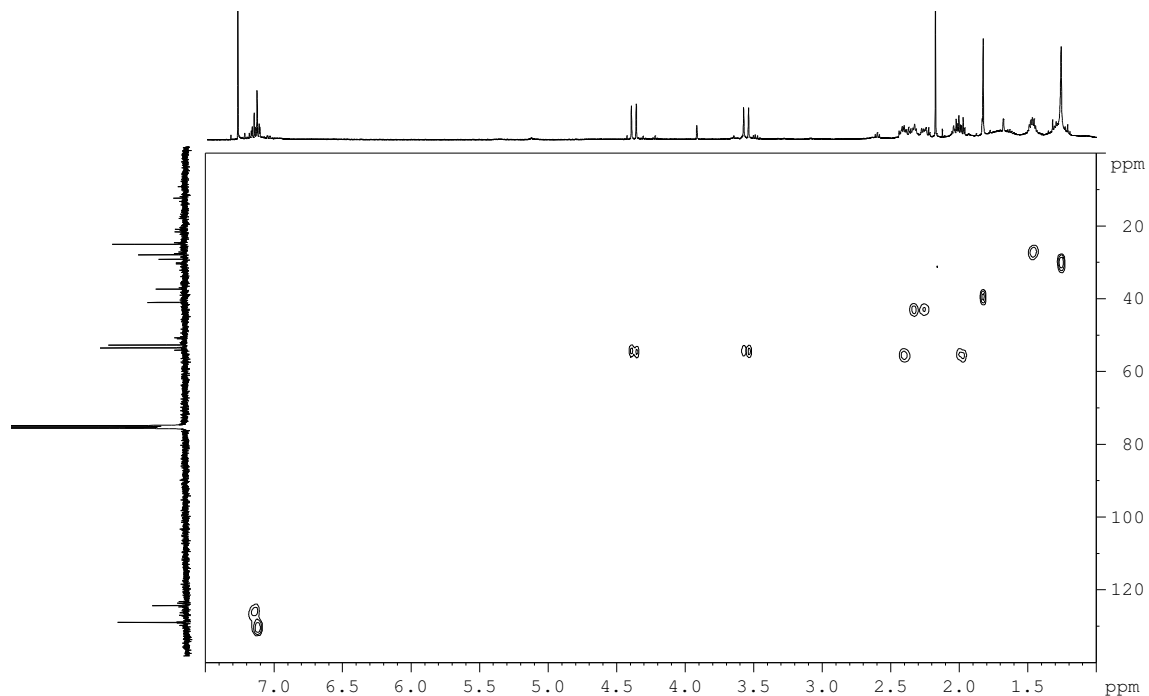


Figure S36. ^1H -NMR spectra of mixture crude of reductive elimination reaction of complex **1I** using 20 equiv. of HPF_6 in CD_3CN , 400MHz at 298 K. Signals labeled (*) correspond to $\text{L}_1\text{-I}(\text{H}^+)$ (85% yield approx).

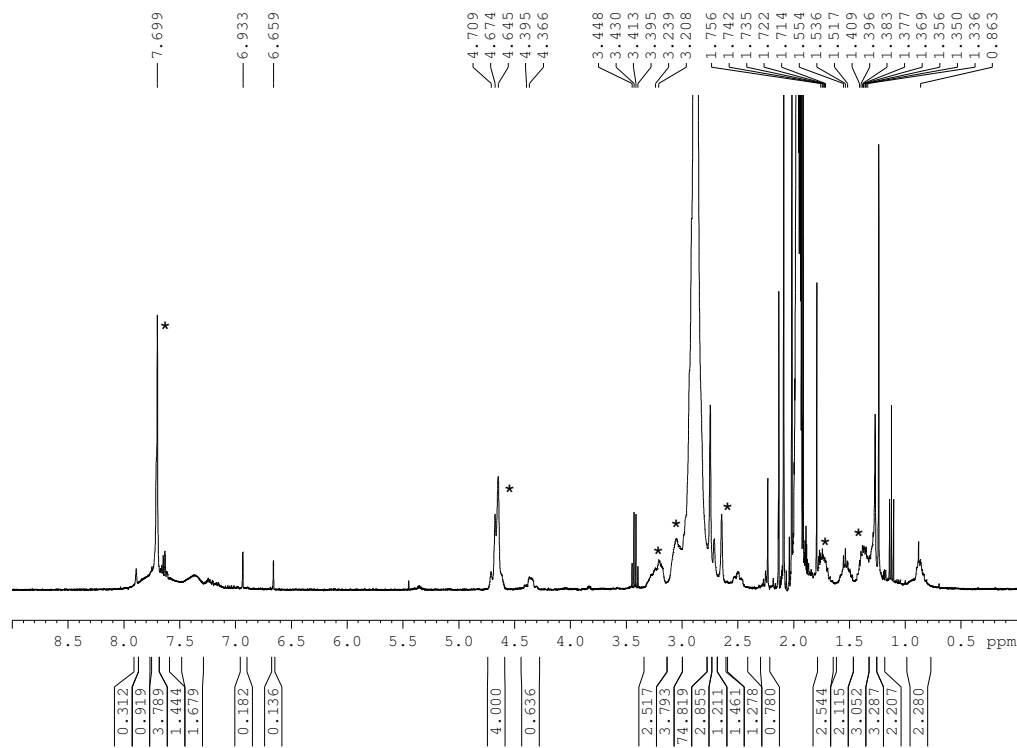


Figure S37. ^1H -NMR spectrum of $\text{L}_2\text{-Cl}$ in CDCl_3 , 400 MHz, at 298 K.

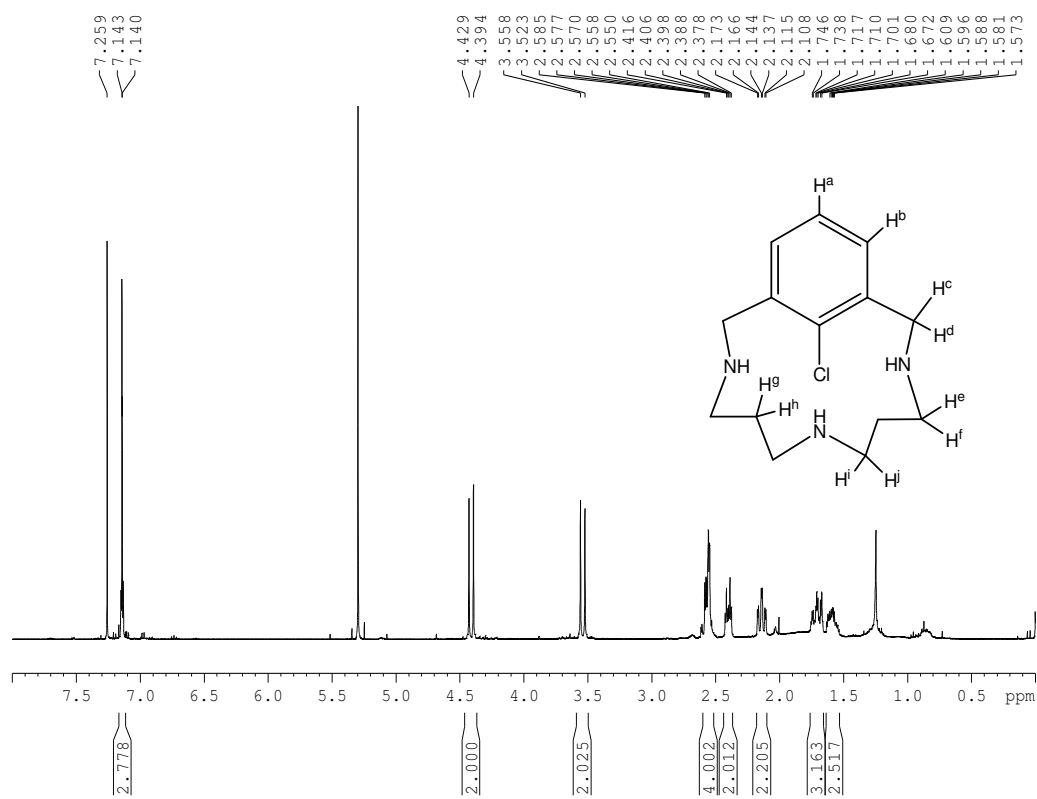


Figure S38. ^{13}C -NMR spectrum of $\text{L}_2\text{-Cl}$ in CDCl_3 , 400 MHz, at 298 K.

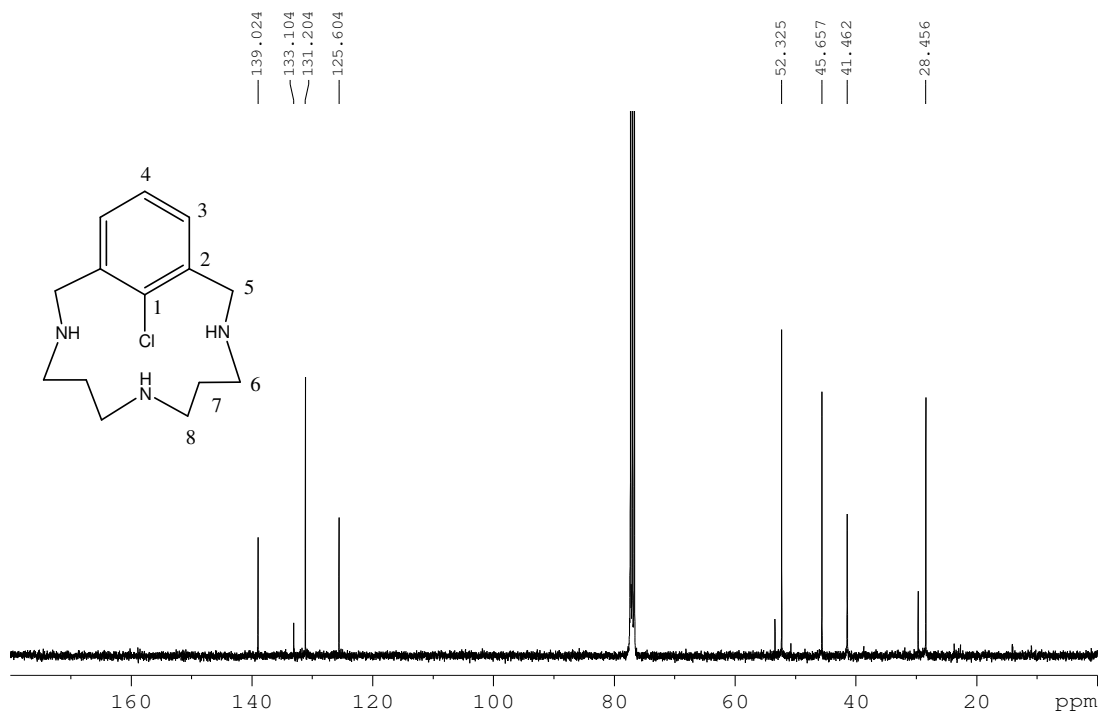


Figure S39. ^1H -NMR spectrum of **L₂-Br** in CDCl_3 , 400 MHz, at 298 K.

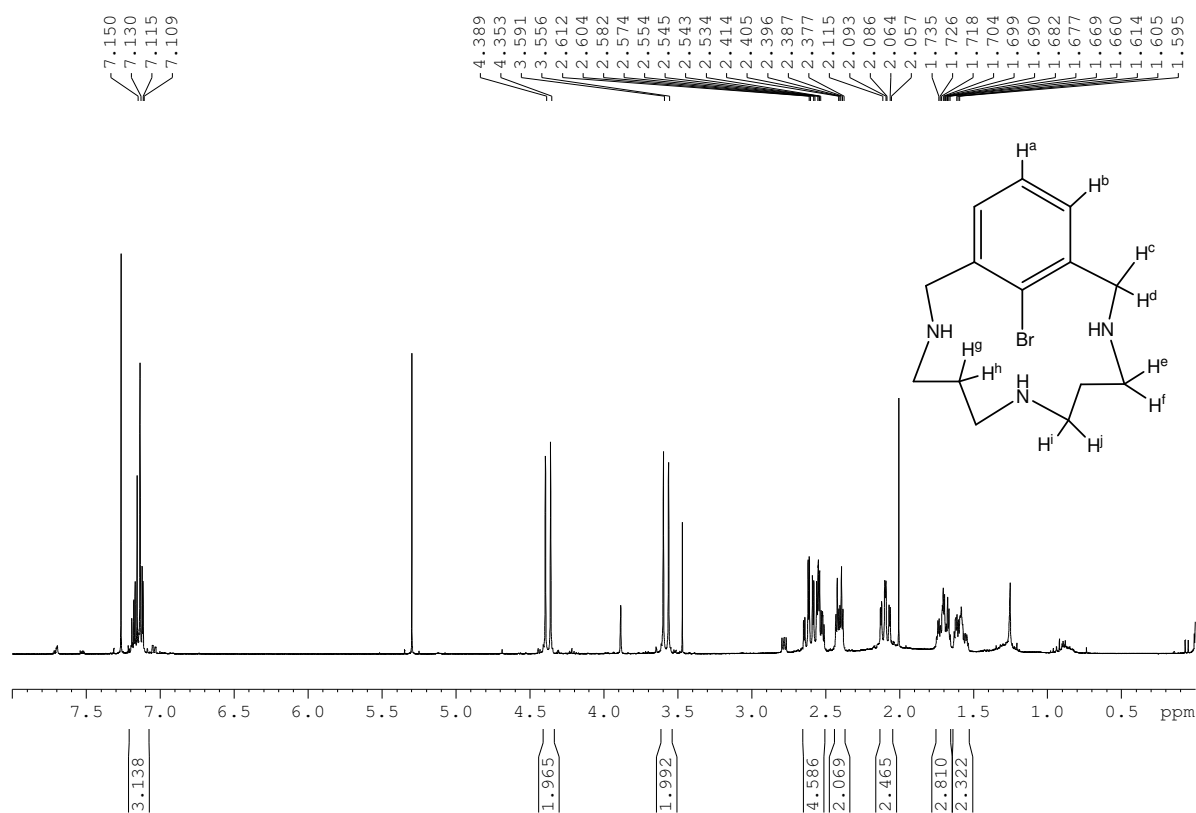


Figure S40. ^{13}C -NMR spectrum of **L₂-Br** in CDCl_3 , 400 MHz, at 298K.

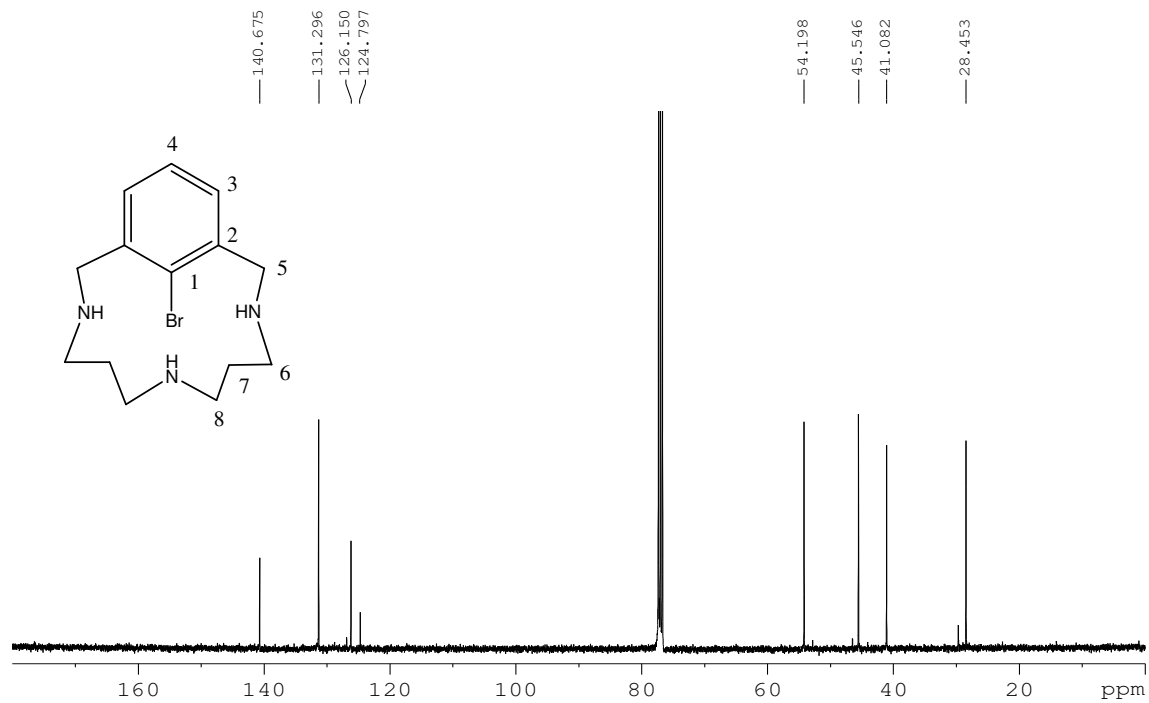


Figure S41. Eyring plot for the reaction of complex **1_{Br}** obtained by monitoring the reaction by UV-visible spectroscopy. Reaction conditions: $[1_{\text{Br}}] = 0.5 \text{ mM}$, $[\text{CF}_3\text{SO}_3\text{H}] = 0.75 \text{ mM}$, CH_3CN , 278-298 K.

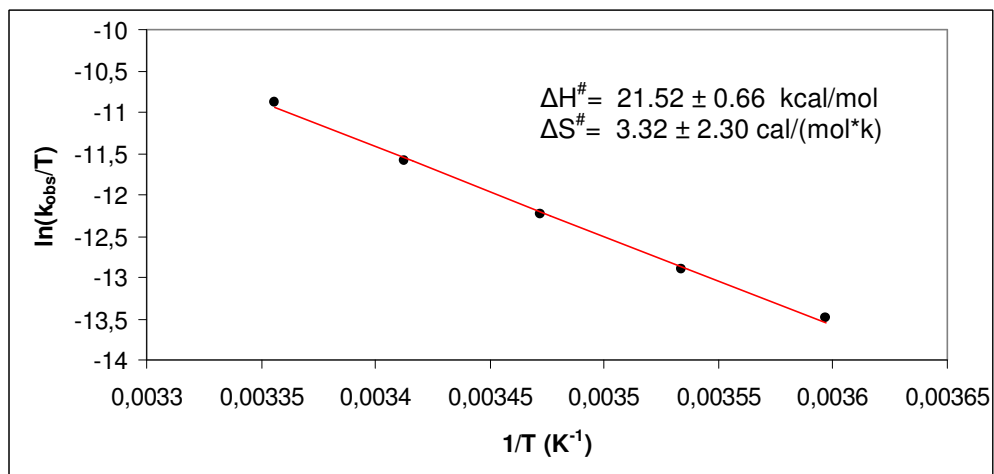


Figure S42. UV-vis monitoring of reductive elimination of complex $[\text{L}_1\text{C}-\text{Cu}^{\text{III}}-\text{Cl}]\text{Cl}$ (**1_{Cl}**) upon addition of 1.5 equivalents of acid ($[\text{1}_{\text{Cl}}] = 0.1 \text{ mM}$, $[\text{CF}_3\text{SO}_3\text{H}] = 0.75 \text{ mM}$, CH_3CN , 283 K). Inset shows decay profile at 374 nm (circles = experimental data, solid-line = first-order theoretical fit).

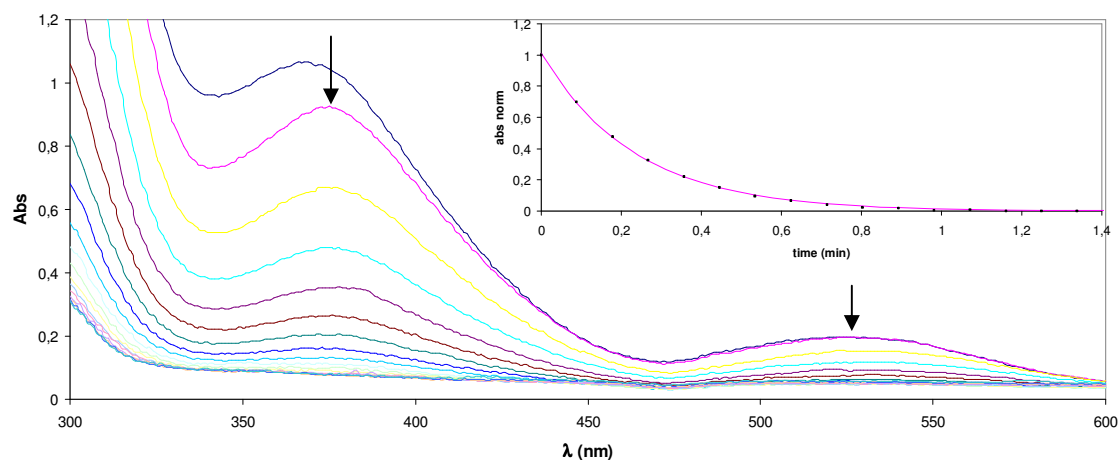


Figure S43. Eyring plot for the reaction of complex **1Cl** obtained by monitoring the reaction by UV-vis spectroscopy. Reaction conditions: $[1_{\text{Cl}}] = 0.5 \text{ mM}$, $[\text{CF}_3\text{SO}_3\text{H}] = 0.75 \text{ mM}$, CH_3CN , 253–283 K.

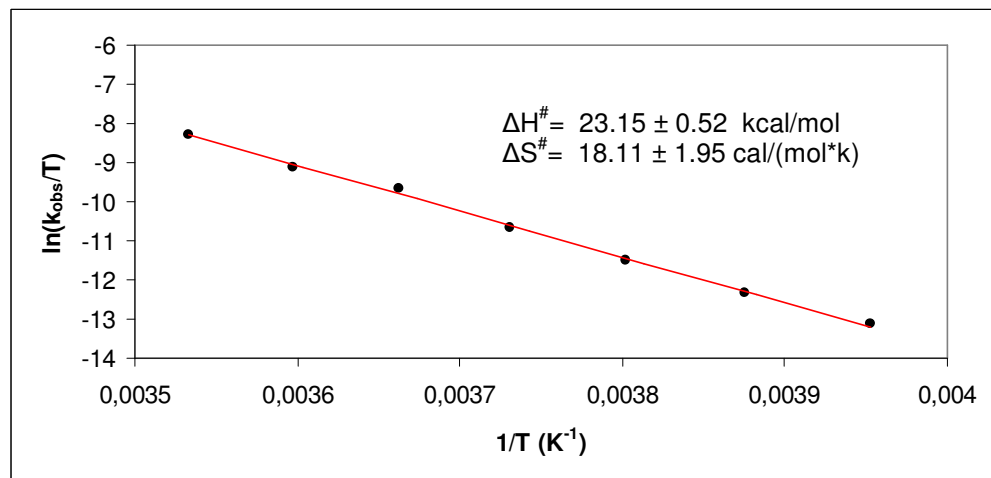


Figure S44. UV-vis monitoring of reductive elimination of complex $[\text{L}_2\text{C}-\text{Cu}^{\text{III}}-\text{Cl}]_{\text{Cl}}$ (**2Cl**) upon addition of 1.5 equivalents of acid ($[2_{\text{Cl}}] = 0.1 \text{ mM}$, $[\text{CF}_3\text{SO}_3\text{H}] = 0.75 \text{ mM}$, CH_3CN , 288 K). Inset shows decay profile at 374 nm (circles = experimental data, solid-line = first-order theoretical fit).

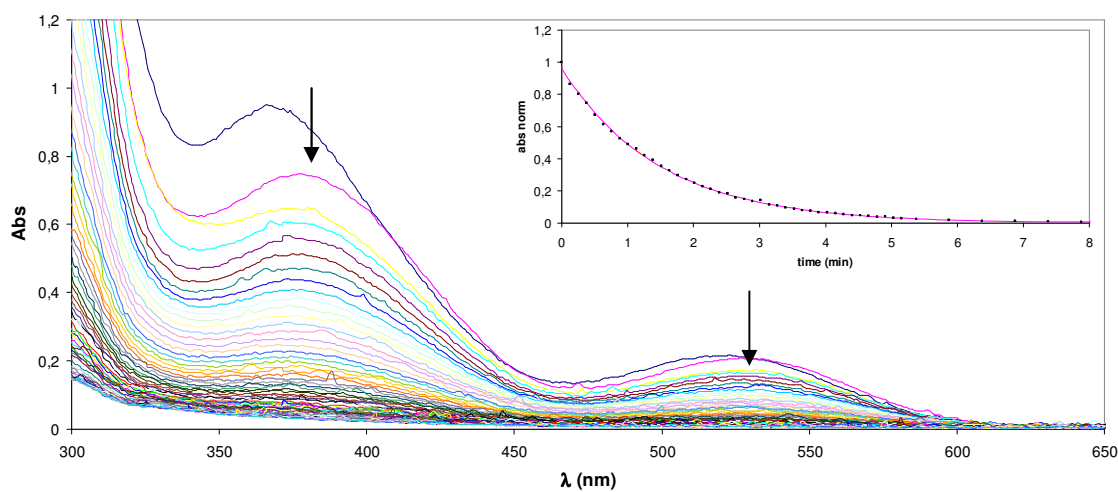


Figure S45. Eyring plot for the reaction of complex **2Cl** obtained by monitoring the reaction by UV-visible spectroscopy. Reaction conditions: $[2_{\text{Cl}}] = 0.5 \text{ mM}$, $[\text{CF}_3\text{SO}_3\text{H}] = 0.75 \text{ mM}$, CH_3CN , 278-298 K.

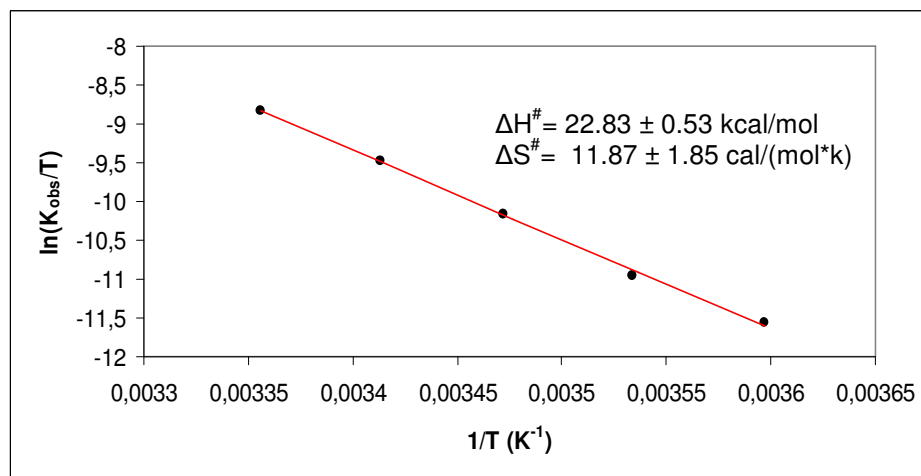


Figure S46. Dependence of k_{obs} on the $[\text{CF}_3\text{SO}_3\text{H}]$ obtained by monitoring the reaction of **1Br** with $\text{CF}_3\text{SO}_3\text{H}$ by UV-visible spectroscopy. Reaction conditions: $[1_{\text{Br}}] = 0.3 \text{ mM}$, $[\text{CF}_3\text{SO}_3\text{H}] = 0.76-4.9 \text{ mM}$, CH_3CN , 297 K.

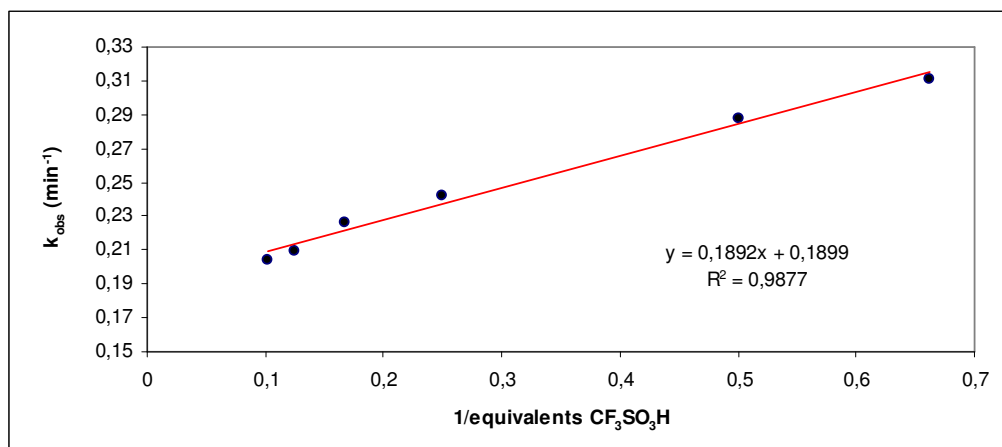


Figure S47. Characterization of complexes **1_{Br}** and **2_{Cl}** by 1D and 2D NMR spectroscopy at 243 K in CD₃CN (black numbers) and adding 1.5 equivalents of CF₃SO₃H (red numbers).

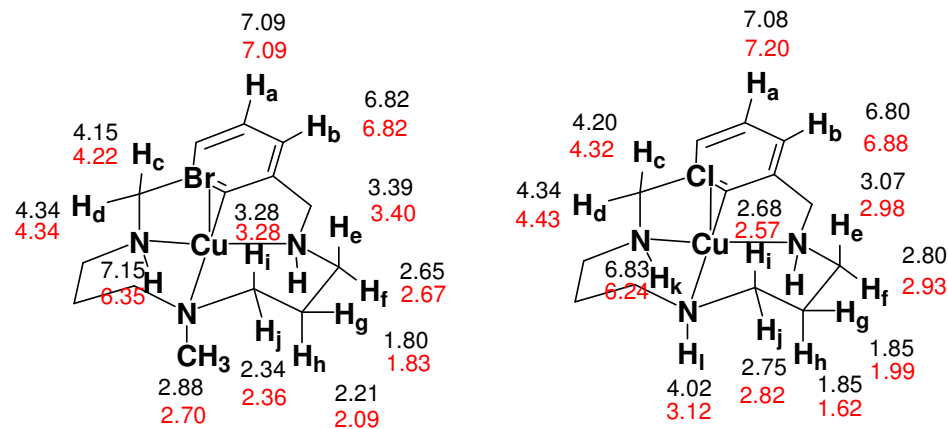


Figure S48. a) ¹H-NMR (600 MHz) spectrum of complex **1_{Br}** at 243 K in CD₃CN (bottom) and after addition of 1.5 equivalents of CF₃SO₃H (top).

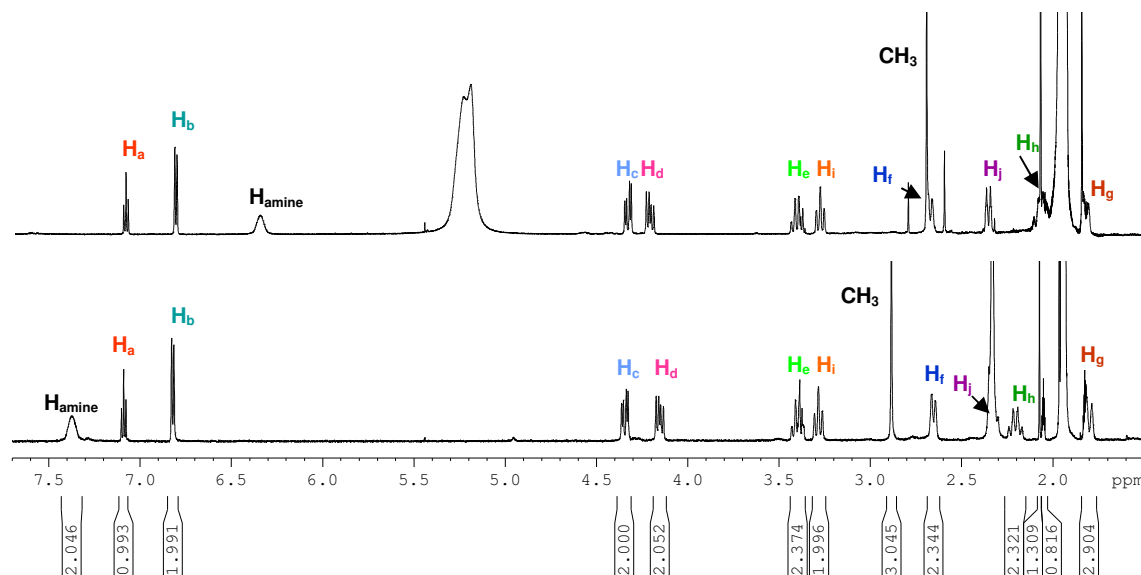


Figure S49. NOESY spectrum of complex **1_{Br}** at 243K in CD₃CN in acid media (1.5 equivalents of CF₃SO₃H).

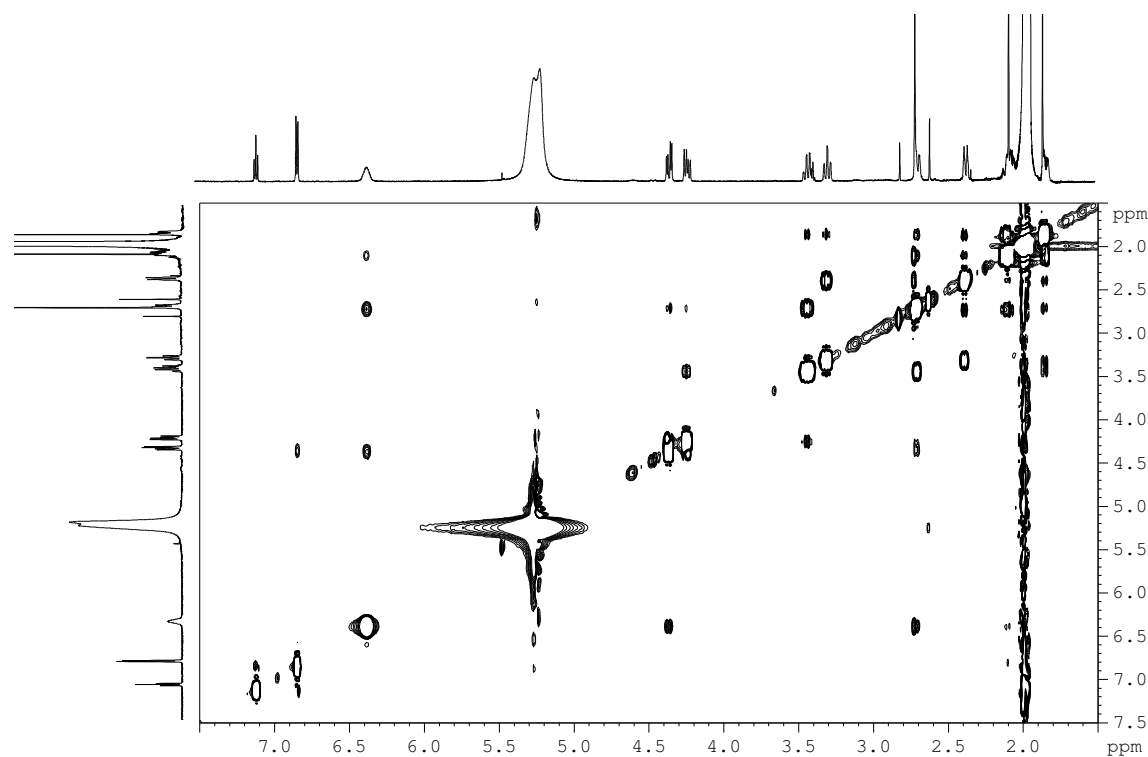


Figure S50. HMBC spectrum of complex **1_{Br}** at 243K in CD₃CN in acid media (1.5 equivalents of CF₃SO₃H).

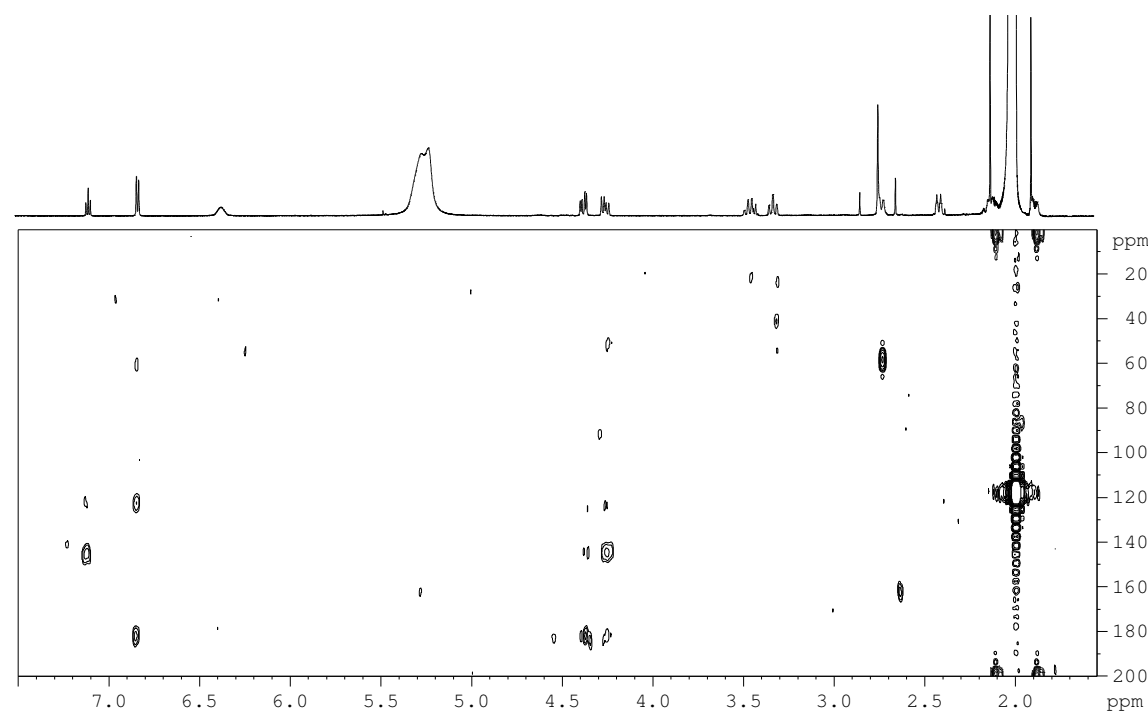


Figure S51. ^1H -NMR spectra of complex $\mathbf{2}_{\text{Cl}}$ at 243 K in CD_3CN (bottom) and after addition of 1.5 equiv. of $\text{CF}_3\text{SO}_3\text{H}$ (top).

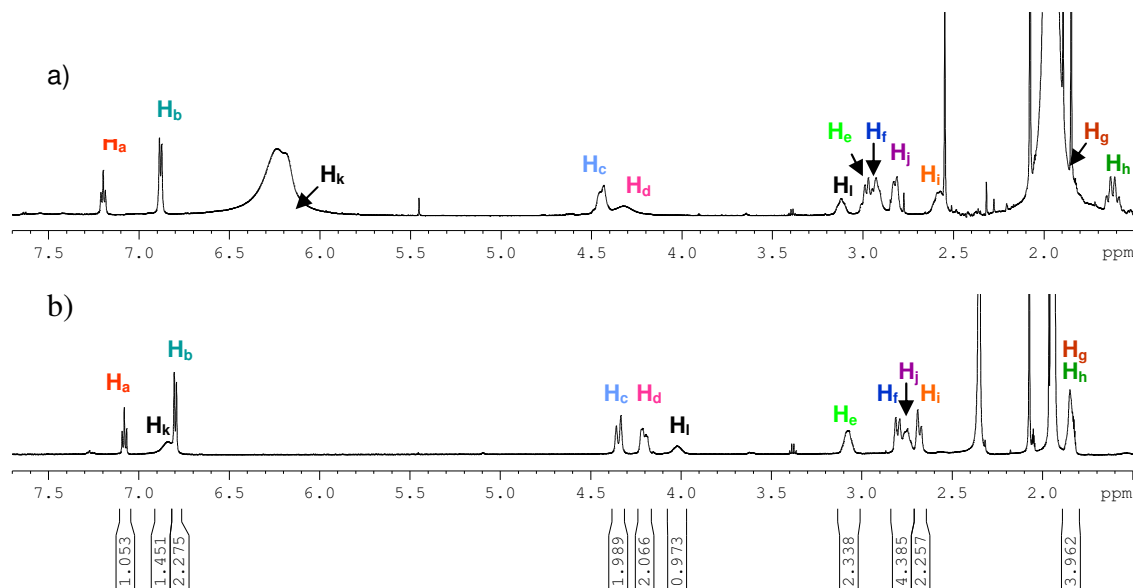


Figure S52. HSQC spectrum of complex $\mathbf{2}_{\text{Cl}}$ at 243 K in CD_3CN in acid media (1.5 equivalents of $\text{CF}_3\text{SO}_3\text{H}$).

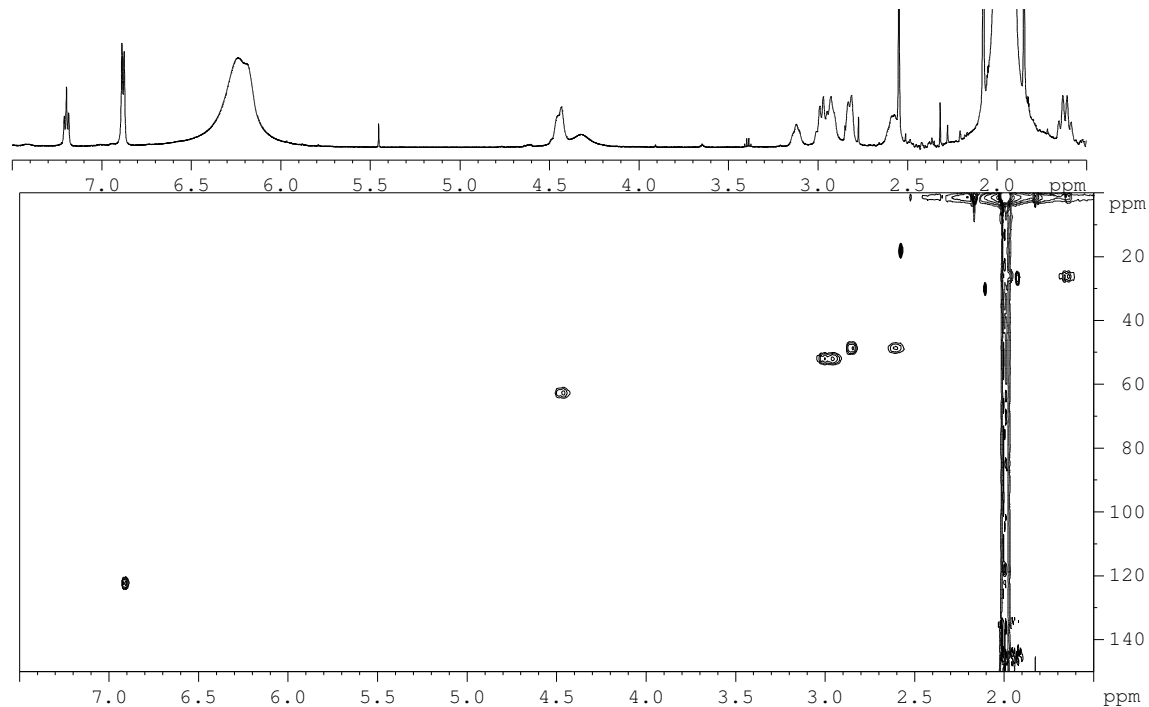
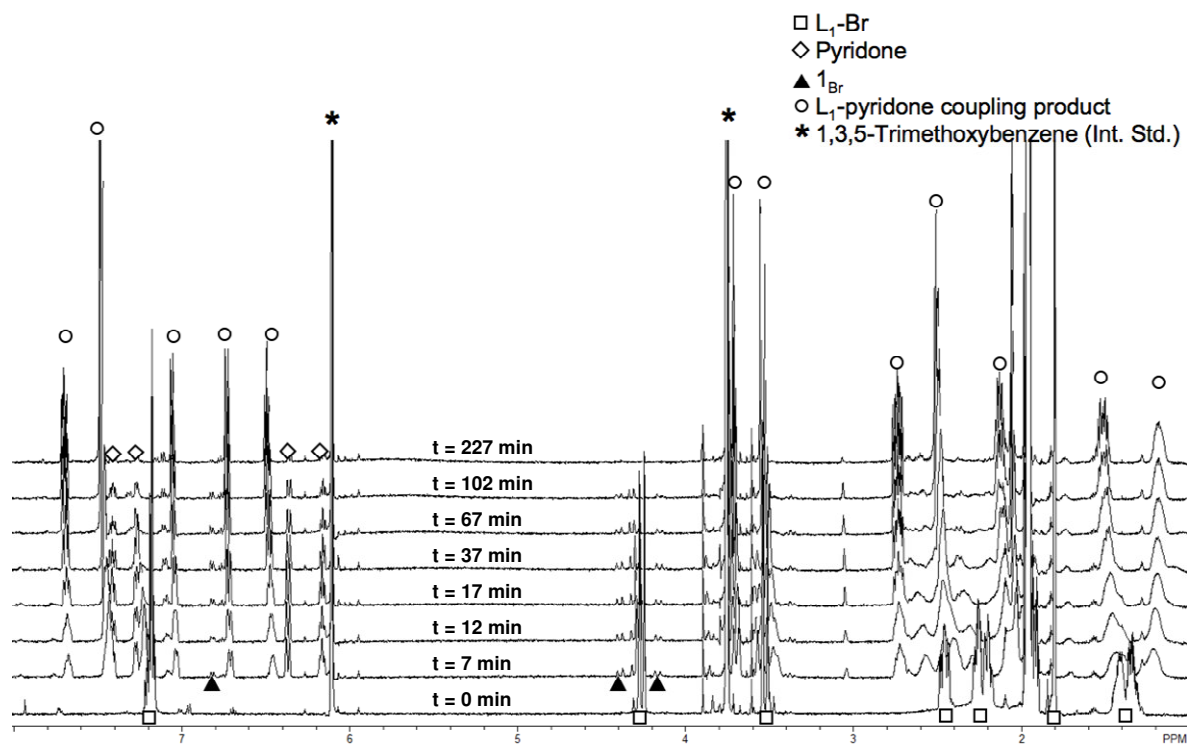


Figure S53. Full scale NMR spectra acquired during the cross-coupling of pyridone with **L₁-Br** catalyzed by 3.3 mol % [Cu^I(CH₃CN)₄]PF₆.



3. Supplementary Tables

Table S1. UV-visible characterization of aryl-Cu^{III}-halide complexes, complex concentration 0.8 mM in CH₃CN at 298 K.

[L ₁ C-CuX]X	λ ₁ (nm)	ε ₁ (M ⁻¹ cm ⁻¹)	λ ₂ (nm)	ε ₂ (M ⁻¹ cm ⁻¹)	[L ₂ C-CuX]X	λ ₁ (nm)	ε ₁ (M ⁻¹ cm ⁻¹)	λ ₂ (nm)	ε ₂ (M ⁻¹ cm ⁻¹)
Cl	369	1409	524	239	Cl	369	1972	521	451
Br	399	1365	550	624	Br	395	1362	545	793
I	422	697	635	1474	I	417	831	621	1955

Table S2. Redox potentials (CV); [L_iC-Cu^{III}-X]= 1mM, scan rate= 0.2 V/s, TBAPF₆ 0.1M, CH₃CN, 263 K, using SSCE as the reference electrode and Fc/Fc⁺ as internal reference.

	E _{1/2} (V) (vs. Fc/Fc ⁺)	E _{pc} (V)	E _{pa} (V)	ΔE (V)	I _{pa} /I _{pc}
1 _{Cl}	-0.33 (0.72)	-0.40	-0.26	0.14	0.7
1 _{Br}	-0.31 (0.69)	-0.37	-0.24	0.13	0.8
1 _I	-0.23 (0.62)	-0.28	-0.17	0.11	0.6
2 _{Cl}	-0.40 (0.79)	-0.46	-0.33	0.13	0.7
2 _{Br}	-0.36 (0.75)	-0.42	-0.30	0.12	0.7
2 _I	-0.29 (0.68)	-0.36	-0.21	0.15	0.9

Table S3. Cathodic reduction potentials (E_{pc}) obtained by cyclic voltammetries of 1_{Cl}, 1_{Br}, 2_{Cl} and 2_{Br} upon addition of 4.5 equiv. of CF₃SO₃H (263K, CH₃CN, [L_iC-Cu^{III}X]X= 1mM, scan rate= 0.2V/s, TBAP 0.1M, using Fc/Fc⁺ as a internal reference).

Complex	E _{pc} (V) neutral media	E _{pc} (V) acid media ^a	anionic shift (V)
1 _{Cl}	-0.40	-0.28	0.12
1 _{Br}	-0.37	-0.30	0.07
2 _{Cl}	-0.46	-0.29	0.17
2 _{Br}	-0.42	-0.35	0.07

Table S4. Crystallographic data and structure refinement for complexes $[L_1C\text{-Cu}^{III}\text{Cl}]Cl$ (**1_{Cl}**), $[L_1C\text{-Cu}^{III}\text{Br}]Br$ (**1_{Br}**), $[L_1C\text{-Cu}^{III}\text{I}]I$ (**1_I**), $[L_2C\text{-Cu}^{III}\text{Cl}]Cl$ (**2_{Cl}**), $[L_2C\text{-Cu}^{III}\text{I}]I$ (**2_I**); the Cambridge Crystallographic Data Centre (CCDC) codes are 735508-735512, respectively.

Compound	1_{Cl}	1_{Br}	1_I	2_{Cl}[·]H₂O	2_I
Empirical formula	$C_{15}H_{24}Cl_2CuN_3$	$C_{15}H_{24}Br_2CuN_3$	$C_{15}H_{24}I_2CuN_3$	$C_{14}H_{24}Cl_2CuN_3O$	$C_{14}H_{22}I_2CuN_3$
Formula weight	380.81	469.73	563.71	380.4	549.69
Temperature, K	300(2)	300(2)	300(2)	300(2)	100(2)
Wavelength, Å	0.71073	0.71073	0.71073	0.71073	0.71073
Crystal system	orthorhombic	Orthorhombic	monoclinic	orthorhombic	triclinic
Space group	Pca21	Pca21	P21/c	Pca21	P-1
Unit cell dimensions					
a, Å	11.892(9)	12.3103(14)	7.1650(6)	12.470(2)	15.441(7)
α , deg	90	90	90	90	66.117(7)
b, Å	15.074(11)	15.3429(17)	17.7756(14)	15.254(7)	16.225(7)
β , deg	90	90	99.2740(10)	90	83.242(8)
c, Å	9.640(7)	9.6916(11)	15.0327(12)	9.0700(17)	16.686(8)
γ , deg	90	90	90	90	70.542(8)
Volume, Å ³	1728(2)	1830.5(4)	1889.6(3)	1725.3(6)	3603(3)
Density (calculated), g·cm ⁻³	1.464	1.704	1.982	1.481	2.026
Cell formula units_Z	4	4	4	4	8
Absorption coefficient, mm ⁻¹	1.570	5.556	4.421	1.577	4.634
Crystal size, mm ³	0.6 x 0.2 x 0.1	0.4 x 0.15 x 0.08	0.4 x 0.4 x 0.2	0.6 x 0.4 x 0.08	0.3 x 0.1 x 0.08
Reflections collected	25418	27574	29056	24670	55714
Independent reflections	4281 [R(int)= 0.0696]	4524 [R(int)= 0.0395]	4675 [R(int)= 0.0392]	4186 [R(int)= 0.0336]	17207 [R(int)= 0.0420]
Final R indices [$I > 2\sigma(I)$]	R1= 0.0330, wR2= 0.0756	R1= 0.0266, wR2= 0.0547	R1= 0.0259, wR2= 0.0615	R1= 0.0455, wR2= 0.1358	R1= 0.0508, wR2= 0.1291
R indices (all data)	R1= 0.0442, wR2= 0.0805	R1= 0.0374, wR2= 0.0576	R1= 0.0367, wR2= 0.0644	R1= 0.0496, wR2= 0.1419	R1= 0.0971, wR2= 0.1489

Table S5. Selected bond lengths [\AA] and angles [$^\circ$] for aryl-Cu^{III}-halide complexes **1_{Cl}**, **1_{Br}**, **1_I**, **2_{Cl}** and **2_I**.

	1_{Cl}	1_{Br}	1_I	2_{Cl}	2_I
Cu-X (X= Cl, Br, I)	2.455 (16)	2.6999 (5)	2.9001 (4)	2.4675 (10)	2.8122 (13)
N1-Cu	1.972 (3)	1.974 (2)	1.972 (2)	1.986 (5)	1.997 (7)
N2-Cu	2.037 (3)	2.034 (2)	2.017 (2)	1.999 (3)	1.996 (6)
N3-Cu	1.971 (3)	1.974 (2)	1.968 (2)	1.974 (4)	1.988 (7)
C1-Cu	1.908 (3)	1.914 (3)	1.905 (3)	1.898 (3)	1.911 (7)
C1-Cu-N1	82.58 (11)	81.69 (12)	81.92 (12)	81.64 (17)	81.5 (3)
C1-Cu-N3	81.78 (12)	82.53 (12)	82.65 (15)	82.25 (16)	81.6 (3)
N1-Cu-N2	95.06 (9)	96.98 (10)	96.46 (10)	96.70 (15)	97.4 (3)
N2-Cu-N3	96.89 (9)	95.17 (9)	95.74 (10)	95.37 (15)	95.2 (3)
C1-Cu-N2	169.39 (10)	169.44 (11)	170.01 (11)	170.06 (15)	169.7 (3)
N1-Cu-N3	155.70 (11)	155.78 (10)	156.78 (11)	152.64 (17)	152.1 (2)

4. Supplementary Notes

1. Ribas, X.; Jackson, D. A.; Donnadieu, B.; Mahía, J.; Parella, T.; Xifra, R.; Hedman, B.; Hodgson, K. O.; Llobet, A.; Stack, T. D. P. *Angew. Chem. Int. Ed.*, **41**, 2991-2994 (2002).
2. Xifra, R.; Ribas, X.; Llobet, A.; Poater, A.; Duran, M.; Solà, M.; Stack, T. D. P.; Benet-Buchholz, J.; Donnadieu, B.; Mahía, J.; Parella, T. *Chem.-Eur. J.*, **11**, 5146–5156 (2005).